



eetac

Escola d'Enginyeria de Telecomunicació i
Aeroespacial de Castelldefels

UNIVERSITAT POLITÈCNICA DE CATALUNYA

TREBALL DE FI DE CARRERA

TÍTOL DEL TFC: Validation activities of a microprocessor for space applications

TITULACIÓ: Enginyeria Tècnica Aeronàutica, especialitat Aeronavegació

AUTOR: Roser Farré Ponsa

DIRECTOR: Dr. Jordi Guitierrez Cabello

DATA: July 20th, 2012

Títol: Activitats per a la validació d'un microprocessador per aplicacions espacials

Autor: Roser Farré Ponsa

Director: Dr. Jordi Gutierrez Cabello

Data: 20 de juliol de 2012

Resum

Enviar un satèl·lit a l'espai és una missió d'alt cost. No obstant, actualment, s'estan construint satèl·lits de massa i mida molt més reduïda per abaratir els costos d'algunes missions espacials, sobretot, les que tenen caire científic i educatiu. Aquesta tesi es focalitza en l'estudi d'un dels components del femtosatèl·lit creat per l'EETAC, el microprocessador.

Per poder dur a terme el requeriment de baix cost, aquets satèl·lits usen tecnologia COTS. Els punts positius d'aquesta tecnologia es que és més econòmica que la usada en satèl·lits comercials i és a l'abast de tothom. Per altra banda, els seu punt negatiu es que no és una tecnologia òptima per operar en espai, ja que no està qualificada i per tant no sabem la seva fiabilitat en aquest ambient.

Un cop presentat el problema existent amb la tecnologia COTS, l'objectiu d'aquesta tesi és assolir un cert nivell de qualificació espacial. La tecnologia COTS que està sotmesa a anàlisis és el microprocessador ATmega 168.

Per poder qualificar el microprocessador, primerament s'analitzen les seves possibles aplicacions i futures missions. Després, es realitza un anàlisis de tota la problemàtica que comporten les diferents fases que experimenta el microprocessador: pre-lançament, llançament i operació en òrbita.

Un cop analitzats tots els efectes que el microprocessador ha de suportar durant una missió, s'estudien els passos per a poder obtenir la qualificació espacial mitjançant els TRL, és a dir, quins TRA s'han de realitzar. A més a més, s'estudia també en quines fases perillarà més el seu rendiment i, finalment, es decideixen els tests corresponents per confirmar el seu funcionament durant la missió. Els tests escollits són: una prova de buit tèrmic i l'estudi de la radiació espacial simulant els cinturons de Van Allen, mitjançant els software FLUKA i SPENVIS. Per poder entendre el comportament del microprocessador en els tests, abans dels experiments i simulacions, es detalla teòricament els dos medi ambient escollits.

Finalment, un cop realitzats els test, es confirmen els TRL que el microprocessador ha superat. Així doncs, el TRL 1 i TRL 2 queden superats, ja que durant el treball es realitza una primera idea de la missió i s'analitzen les possibles aplicacions. El TRL 3 també s'assoleix, ja que supera tots els test i simulacions proposats. No obstant, el TRL 4, degut a que incorpora integració amb altres components del femtosatèl·lit, queda fora del nostre abast.

Title: Validation activities of a microprocessor for space applications

Author: Roser Farré Ponsa

Director: Dr. Jordi Gutierrez Cabello

Date: July, 20th 2012

Overview

Launching a satellite is a high cost mission. However, nowadays, low-mass and low-cost satellites are being developed to reduce mission costs, above all the scientific and educative ones. This thesis focuses on the study of one of the components of a femtosatellite designed and build at EETAC university. The component to be analyzed is the microprocessor.

In order to meet the low cost requirements, those satellites must be built with COTS technology. The positive point of that technology is that it is affordable to anyone, in terms of economical aspects and readily availability. Nevertheless, it is not optimum to operate in the space environment, since it is not qualified and thus, its survivability is unknown.

Once the existent problem of the COTS technology has been presented, the goal of this thesis is to achieve a certain space qualification level. The microprocessor Atmega 168 will be the analyzed COTS component.

Future missions and potential applications are firstly analyzed in order to space-qualify the microprocessor. After that, the issues regarding to all the mission phases (pre-launch, launch, and orbit operations) are studied. This will help us to determine what are the harmful effects on the microprocessor.

When all the effects that the microprocessor must deal with have been analyzed, the steps to obtain a certain space qualification are addressed. The basic procedures are defined by the corresponding TRA for each TRL. From TRA documentation, the proper tests and simulations are chosen within a realistic environment. The tests are a thermal vacuum laboratory experiment and a radiation exposure analysis, simulating the Van Allen belts, using the commercial software packages FLUKA and SPENVIS. Theoretical background to support the experiments and simulations are previously provided.

Finally, after testing the microprocessor, the TRL level reached by it can be determined. Therefore, TRL 1 and TRL 2 are clearly achieved, since potential applications of the physical concept are developed. Given all that, we can conclude that the microprocessor has achieved TRL level 3. It passed all the tests and simulations conducted in this thesis. Nonetheless, TRL 4 is not achievable because Integration between satellite components must be tested. The integration of components is out of the scope of this thesis.

Al iaío,

*perquè des de la distància,
sempre hi has estat present...*

ACKNOWLEDGEMENTS

Aquestes línies del projecte van dedicades a totes les persones que m'han acompanyat durant molt temps i, d'una forma o altra, n'han fet possible la seva realització.

En primer lloc, agraeixo al meu supervisor, en Jordi Gutierrez Cabello, tota l'ajuda proporcionada durant el temps que hem estat treballant en aquest projecte, per guiar-me en el seu desenvolupament i proporcionar-me tot el suport tècnic necessari.

Vull donar les gracies a la meva família, especialment, als meus *Pares* i al meu *germà* per tot el suport que m'han donat sempre, ajudant-me en tot el que han pogut i més. Els agraeixo profundament aquesta gran confiança que tenen en mi, no sabeu l'important que arriba a ser, gracies a vosaltres ha estat possible.

Finalment, vull agrair als amics que m'han acompanyat durant aquests anys. Primerament agrair-li al Javi el fet d'haver estat sempre al meu costat, saps que sense tu tot hagués estat més complicat. També vull dedicar aquesta tesi a la Sara, l'Alba, en Carlos, la Sandra i en Javi S., amb ells he passat grans moments que no oblidaré mai. Espero que la nostra amistat perduri en el temps.

Roser Farré i Ponsa

Barcelona, Juliol 2012

CONTENTS

CHAPTER 1. INTRODUCTION	1
1.1. Motivation	1
1.2. Outline of Thesis	2
CHAPTER 2. SPACE SYSTEM AND MISSION REQUIREMENTS	3
2.1. Space System	3
2.2. Mission Requirements	5
CHAPTER 3. SPACE ENVIRONMENT ANALYSIS	7
3.1. Pre-launch Phase Environment	7
3.2. Launch Phase Environment	7
3.2.1. Acoustic Vibration Environment	8
3.2.2. Launch Acceleration.....	8
3.2.3. Mechanical Shock	8
3.2.4. Thermal Environment.....	8
3.2.5. Atmospheric Pressure.....	8
3.2.6. Electromagnetic Interference	9
3.3. Space Phase Environment	9
3.3.1. The Vacuum Environment.....	9
3.3.2. The Neutral Environment	9
3.3.3. The Plasma Environment.....	10
3.3.4. The Radiation Environment.....	11
3.3.5. The MM/OD.....	13
CHAPTER 4. PROCEDURES AND MECHANISMS TO QUALIFY COMPONENTS FOR SPACE TECHNOLOGY	15
4.1. Technology Readiness Level	16
4.2. Technology Readiness Assessments	19
4.3. Conducted Experiments	21

CHAPTER 5. SPACE TECHNOLOGY QUALIFICATION: THEORETICAL BACKGROUND	23
5.1. Vacuum Exposure Analysis	23
5.1.1. Pressure	23
5.1.2. Solar UV	24
5.1.3. Molecular Contamination	24
5.1.4. Particulate Contamination	25
5.2. Radiation Exposure Analysis	26
5.2.1. TD Effects in Aerospace	26
5.2.2. TID	28
5.2.3. SEE	29
CHAPTER 6. SPACE TECHNOLOGY QUALIFICATION: EXPERIMENTAL TESTS	35
6.1. Vacuum Test	35
6.2. Temperature Test	36
6.3. Radiation Test.....	37
6.3.1. FLUKA.....	38
6.3.2. SPENVIS.....	47
6.3.3. Conclusions.....	50
CHAPTER 7. CONCLUSIONS AND FUTURE WORK	53
7.1. Conclusions.....	53
7.2. Future Work	54
BIBLIOGRAPHY	55
APPENDIX A.....	57
APPENDIX B.....	59

LIST OF FIGURES

Fig. 2.1 Arduino PRO MINI.....	4
Fig. 3.1 The different layers of the atmosphere.....	10
Fig. 3.2 The LEO plasma density as a function of altitude.....	11
Fig. 3.3 The Earth's magnetosphere	12
Fig 3.4 Variation in cosmic rays due to the solar cycle.	13
Fig. 4.1 Generic TRA steps	19
Fig. 5.1 Atmospheric pressure versus altitude.	23
Fig. 5.2 Atmospheric absorption.....	24
Fig. 5.3 Residence time of contaminants.	25
Fig. 5.4 Variation of the computed annual dose on circular orbits as a function of altitude.....	28
Fig 5.5 The relative abundances of all of the ions in cosmic rays. They are plotted in terms of the peak flux in their energy spectra.....	31
Fig. 5.6 Relationship between the dipole and cutoff rigidity to determine the particle energy required to penetrate the magnetosphere.....	31
Fig. 5.7 Integral LET spectra for galactic cosmic rays during solar maximum and solar minimum.	32
Fig. 5.8 Variation of LET spectra with inclination for LEO.....	32
Fig. 5.9 Effect of shielding on cosmic ray LET spectra.	33

Fig. 5.10 Total exposure to trapped protons as a function of altitude and inclination for circular orbits.	34
Fig. 5.11 Proton spectrum in low earth orbit showing the effect of aluminum shielding.....	34
Fig.6.1 Thermic Vacuum Chamber	35
Fig. 6.2 Final test results	36
Fig. 6.3 Thermic Source	37
Fig.6.4 FLUKA Total Equivalent Dose in 1mm Si (from -0,05 cm to 0,05 cm), electron beam. a) 2D projection, seen from Z axe. b) 2D projection, seen from Y axe. c) 1D projection, boxes. d) 1D projection, steps.	39
Fig.6.5 FLUKA Total Equivalent Dose in 1mm Si (from 0 to 0,1cm) and 1mm Al (from -0,1 to 0 cm), electron beam. a) 2D projection, seen from Z axe. b) 2D projection, seen from Y axe. c) 1D projection, boxes. d) 1D projection, steps.....	40
Fig.6.6 FLUKA Total Equivalent Dose in 1mm Si (from 0 to 0,1 cm) and 1mm Cu (from -0,1 to 0 cm), electron beam. a) 2D projection, seen from Z axe. b) 2D projection, seen from Y axe. c) 1D projection, boxes. d) 1D projection, steps.....	41
Fig.6.7 FLUKA Total Equivalent Dose in 1mm Si (from 0 to 0,1 cm) and 2mm Al (from -0,2 to 0 cm), electron beam. a) 2D projection, seen from Z axe. b) 2D projection, seen from Y axe. c) 1D projection, boxes. d) 1D projection, steps.....	42
Fig.6.8 FLUKA Total Equivalent Dose in 1mm Si (from 0 to 0,1cm) and 5mm Al (from -0,5 to 0 cm), electron beam. a) 2D projection, seen from Z axe. b) 2D projection, seen from Y axe. c) 1D projection, boxes. d) 1D projection, steps.....	43
Fig.6.9 FLUKA Total Equivalent Dose in 1mm Si (from -0,05 to 0,05 cm), proton beam. a) 2D projection, seen from Z axe. b) 2D projection, seen from Y axe. c) 1D projection, boxes. d) 1D projection, steps.....	44
Fig.6.10 FLUKA Total Equivalent Dose in 1mm Si (from 0 to 0,1 cm) and 1mm Al (from -0,1 to 0 cm), proton beam. a) 2D projection, seen from Z axe. b) 2D projection, seen from Y axe. c) 1D projection, boxes. d) 1D projection, steps.....	45
Fig. 6.11 FLUKA Total Equivalent Dose in 1mm Si (from 0 to 0,1 cm) and 2mm Al (from -0,2 to 0 cm), proton beam. a) 2D projection, seen from Z axe. b) 2D projection, seen from Y axe. c) 1D projection, boxes. d) 1D projection, steps.....	46
Fig. 6.12 FLUKA Total Equivalent Dose in 1mm Si (from 0 to 0,1 cm) and 5mm Al (from -0,5 to 0 cm), proton beam. a) 2D projection, seen from Z axe. b)	

2D projection, seen from Y axe. c) 1D projection, boxes. d) 1D projection, steps..... 47

Fig. 6.13 SPENVIS, electron beam simulations. a) Total Ionizing Dose in 1mm Si, b) Total Ionizing Dose in 1mm Al (layer 2) and 1mm Si (layer 3), c) Total Ionizing Dose in 2 mm Al (layer 2) and 1mm Si (layer 3), d) Total Ionizing Dose in 5 mm Al (layer 2) and 1mm Si (layer 3). 48

Fig. 6.14 SPENVIS, proton beam simulations. a) Total Ionizing Dose in 1mm Si, b) Total Ionizing Dose in 1mm Al (layer 2) and 1mm Si (layer 3), c) Total Ionizing Dose in 2 mm Al (layer 2) and 1mm Si (layer 3), d) Total Ionizing Dose in 5 mm Al (layer 2) and 1mm Si (layer 3). 49

LIST OF TABLES

Table 2.1 Arduino Main Features	4
Table 4.1 The basic technology readiness levels.....	16
Table 4.2 Summary of independent review and validation processes.	20
Table 6.1. Characteristics of the used physical models	37
Table 6.2 Original Results	50
Table 6.3 Normalized Results	50
Table 6.4 Final Total Dose results.....	50

ACRONYMS

AO	Atomic Oxygen
COTS	Commercial-Off-The-Shelf
DD	Displacement Damage
CMOS	Complementary Metal-Oxide-Semiconductor
DDT&E	Design, Development, Test and Evaluation
EETAC	Escola d'Enginyeria Telecomunicació i Aeroespacial de Castelldefels
EMI	Electromagnetic Interference
ESA	European Space Agency
GCR	Galactic Cosmic Rays
GEO	Geostationary Earth Orbit
GLONASS	Global Navigation Satellite System
GPS	Global Positioning System
ISO	International Standards Organization
LEO	Low Earth Orbit
LET	Linear Energy Transfer
MIPS	Mega-Instruction per Second
MM	Micrometeoroid
MM/OD	Micrometeoroid / Orbital Debris
MOSFET	Metal Oxide Semiconductor Field Effect Transistor
MTBF	Mean Time Between Failure
NASA	National Aeronautics and Space Administration
NSF	National Science Foundation
OD	Orbital Debris
SAA	South Atlantic Anomaly
SEB	Single Event Burn-out
SEE	Single Event Effects
SEL	Single Event Latchup
SEP	Solar Energetic Particles
SEU	Single Event Upset
SPENVIS	Space Environment Information System
Sv	Sievert
R&D	Research and Development
TD	Total Dose
TID	Total Ionizing Dose
TRA	Technology Readiness Assessments
TRL	Technology Readiness Levels
USA	United States of America
USSR	Union of Socialist Soviet Republics
UV	Ultraviolet

CHAPTER 1. INTRODUCTION

1.1. Motivation

Satellites are engineering systems placed in orbit around astronomical objects, such as the Earth, the Moon or the Sun. The first satellite, dating back to 1957, was created by Union of Socialist Soviet Republics (USSR), and named Sputnik.

Satellites have many different applications. We can pick up firstly the scientific ones, such as astronomical observation or Earth characterization. For scientific reasons, typically, space probes observe their targets by means of very advanced sensors and specific instrumentation to collect valuable information of the object. Another application is the telecommunication market. Since the very beginning, experts saw space communications as an efficient way to provide services such as TV services or long-distance fixed and mobile phone calls. Nowadays, they have expanded their business into the Internet services. Another commercial application of satellite systems stands on the navigation sector, where the Global Positioning System (GPS), and its competitors (Russia's Global Navigation Satellite System (GLONASS) and Europe's Galileo constellations) have become the principal navigation standards used worldwide. Nevertheless, satellites have other kind of applications, from the military to educational ones.

Satellites can be divided into different classes regarding its mass. Common satellites have a wet mass (thus including propellants and consumables) of 500 kg or above. A satellite in the 100 to 500 kg range of mass is called a minisatellite, while the ones with masses between 10 kg and 100 kg are called microsattelites. The research group on space engineering at the Escola Enginyeria de Telecomunicació i Aeroespacial de Castelldefels (EETAC) is interested in satellites with total mass in the range of 1-10 kg which belong to the nanosatellite class, picosatellite class, with masses between 0.1 kg and 1 kg, and femtosatellite class masses below 0.1 kg. They have created different satellites for research purposes, including the femtosatellite used along this thesis.

The femtosatellite is based on Commercial-Off-The-Shelf (COTS) technology. COTS technology and products are commercially available and no specific and new technology is needed. By means of using this suite of technologies, the final cost of the femtosatellite can be considerably reduced.

Space environment is an unpleasant place for satellites: they have some troubles to resist in these difficult conditions. Satellites can suffer important problems on their hardware that can make them not work within optimum performances. Due to small size of femtosatellites and launch weight constraints, it is very costly to protect them with strong isolation systems, since isolation is usually based on adding layers of materials. As a consequence, unprotected satellites have a relatively short lifetime. In order to increase the lifetime of satellites, space qualified hardware may be used. To make the hardware be so, it must be first evaluated and it has to achieve a certain Technology Readiness Level (TRL) depending on the mission purpose.

TRLs [1] is a systematic metric measurement system that supports assessments of the maturity of a particular technology and the consistent comparison of maturity between different types of technology.

The main goal of this dissertation is to advance in the TRL metrics of one of the most important component of the femtosatellite created at the EETAC i.e., the microprocessor. The microprocessor employed is an ATmega 168 [2], mounted on an Arduino PRO MINI board [3].

1.2. Outline of Thesis

Chapter 2 provides a detailed description of the space systems. The COTS technology to be analyzed, i.e., Atmega 168 processor mounted on an Arduino PRO MINI board, is presented, showing the main features of it. Finally, potential future missions for the satellite are presented.

In chapter 3, we analyze the physical effects that arise on all the mission phases, (pre-launch, launch, and orbit operations) to well understand the problems that may affect the proper function of the microprocessor.

Chapter 4 presents the procedures needed to space qualify a component. The list of TRL levels used by ESA is exposed and a detailed explanation is included. A general framework to assess the readiness of a given technology is addressed. After presenting the theory, the laboratory experiments and simulations to be carried out are presented.

In chapter 5 we provide with technical background to be able to understand the results of the experiments, in case the reader is not familiar with the topics.

Chapter 6 presents the experimental tests and simulations performed to achieve a certain TRL level. Commercial software FLUKA and SPENVIS are used to analyze the radiation effects.

Finally, chapter 7 concludes the thesis and presents some future works.

CHAPTER 2. SPACE SYSTEM AND MISSION REQUIREMENTS

In this chapter we introduce the principal features of the space system and address the mission requirements. In the first part, we cover the general aspects of the satellite. Then, the microprocessor is introduced. In the second part, we specify current mission requirements. Although the list is incomplete (reflecting its current state of development), we show some possible applications with its basic requirements.

2.1. Space System

The advances in the last two decades in consumer microelectronics have opened a whole new realm of low mass, low cost, and low power applications. In the space area, this has allowed the development of very small, yet quite capable satellites. This evolution let us today to design and implement satellites with total masses below 100 grams, the so-called femtosatellite class.

There are some research groups interested in the femtosatellite market. For instance, the research group at the EETAC has been working on this sector. This group had built a model of just 16.6 grams in mass. Nevertheless, this is not the smallest femtosatellite so far, as the Sprite satellite (Cornell University, United States of America (USA)) is just 4.7 grams, and is being tested in space -attached to the external hull of the International Space Station.

EETAC research group is not only interested in femtosatellites but also on mini-launchers. These launchers are adapted to femtosatellite's weight and performances. Therefore, femtosatellites can be placed in orbit by its own launcher and they don't need a piggyback launch (a piggyback payload launch utilizes the excessive launch capability of a rocket to launch small satellites that are made by a private company or university). The aim is to expand the base of space development and utilization providing an easy and quick launch and operation opportunities for small satellites. Nevertheless, piggyback has high costs compared with a mini-launcher. Moreover, the piggyback constrains are too restrictive for some femtosatellite's future missions. However, it is out of the scope of this thesis the analysis of these mini-launchers. For a complete description of mini-launcher design see [4].

The technology that has allowed manufacturing femtosatellites based on micro-electromechanical systems (MEMS), which up to now have been very seldom used in space applications. This is due to the fact that, well to the contrary of the layman expectations, space qualified technology use to be very robust, but not very state-of-the-art. Very Large Scale Integration (VLSI) microelectronics has not been yet tested in the relevant conditions to ensure their survivability in space conditions. As it is stated before, to evaluate the technological maturity of systems, devices and components, the space community has defined the figure of merit Technology Readiness Level (TRLs, see Chapter 4). Most of the MEMS technology is still in TRL 2 [1] or below.

The main purpose of this project is to keep the mission cost as low as possible. To solve this issue COTS technology is implemented. COTS-based satellites are built only with existing technology mostly based on commercial electronic components. Contrarily, common mission satellites are based on very costly space-qualified technology.

EETAC's femtosatellite is completely built with COTS technology. In this thesis we only analyze its microprocessor, the ATmega 168 from ATMEL Corporation, depicted in Fig. 2.1. It is mounted on an Arduino PRO MINI board that is also formed by other components as shown in the Figure [2].

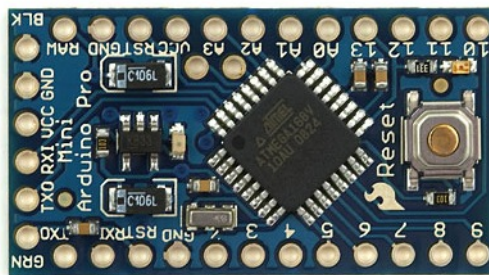


Fig. 2.1 Arduino PRO MINI

Table 2.1 shows the main features of the processor.

Table. 2.1 Arduino Main Features.

Feature	Value
Operating voltage	3.3 V
Flash memory	16 KB
SRAM	1 KB
EEPROM	512 bytes
Clock speed	8 MHz
MIPS	Up to 16 MIPS
Write/Erase cycles	10,000 Flash/100,000 EEPROM
Temperature	-40°C to 85°C

Despite of its small size, this simple processor is capable of 16 Mega-Instruction per Second (MIPS). Unfortunately, it has never been flown to space, and thus it has not achieved any advanced TRL level.

Nevertheless, prior studies have tested its behavior in very high altitude balloon flights (at maximum heights of 35 km), where it has proven flawlessly. However, the conditions of these flights still bear little resemblance with the space environment. For that reason in this dissertation the microprocessor will be tested under space conditions in order to improve its TRL level.

2.2. Mission Requirements

The requirements of the final mission are not defined since the femtosatellite is still under development. Therefore, we are not able to know exactly its high-level requirements, such as coverage, availability, mission geometry, ground systems or payload. Nevertheless, there exists a constraint on the total mission to be low-cost. As a result, all the requirements must be selected such that they satisfy the cost budget.

Generally, designing a space mission is a costly operation, and the satellite cost in orbit is about 10.000-30.000 \$/kg. As we can see, the extremely high cost restricts the number of satellites to be launched continuously, their applications and also reduces the number of competing corporations. Additionally, to optimize satellite performance with cost constraint, they must be designed specifically for each particular mission. Thus, the cost increases due to non-serial manufacturing. As we saw in the previous section, COTS technology may be used to achieve the low-cost mission requirement, and to standardize the design and construction of satellite subsystems.

The missing extended list of mission requirements will be studied in the near future once the needed technology has been developed and tested properly. They may be included in future bachelor thesis that will continue the work presented in this report.

Even though mission requirements are not yet defined, we present some potential applications of interest for the mentioned satellite. As example, we could use the femtosatellite to determine the atmospheric density in the altitude interval of 100-250 km. To do so, the femtosatellite would require including a 3D accelerometer to measure the deceleration produced by the atmospheric drag. Other examples involve the study of natural disasters, such as volcano eruptions or earthquakes. They may be addressed by means of frequent Earth observation using these kinds of satellites launched upon request (responsive space solutions). The analysis and evaluation of the evolution of a natural disaster could be carried out launching a constellation of femtosatellites. They would allow having a frequent control of the zone. As a consequence of that, the satellites have to be previously manufactured before they are needed, since they must be put into orbit in a few hours. Orbits should be Low Earth Orbit (LEO) and they should cover a specific Earth zone. Moreover, more ambitious projects may be accomplished with these small satellites. For instance, the study of the magnetosphere would require launching a collection of femtosatellites at different altitudes to capture the characteristics of the Earth magnetic field. They would need a specific payload based on high-sensitive magnetometers and radiation sensors.

CHAPTER 3. SPACE ENVIRONMENT ANALYSIS

In this chapter, we perform an analysis of all the environments encountered by a spacecraft. It gives a brief summary of [6, 7] that aims to provide the basic ideas to the reader that is not familiar with this subject. For a more detailed explanation the interested reader is referred to [6, 7].

Space travel is hampered not only by the difficulty of getting a spacecraft into orbit, but also by the fact that spacecraft must be designed to operate in environments that are quite different from those found on the Earth's surface. Although it is often considered near perfect vacuum, the type of "space" that is encountered by an orbiting spacecraft may contain significant amounts of neutral molecules, charged and μm -sized particles, and electromagnetic radiation. Each of these environments has the potential to cause severe interaction with spacecraft surfaces or subsystems and they may, if not anticipated, severely impact mission effectiveness.

Before considering the environment in detail, it should be noted that the different phases in the life of a space vehicle, namely, manufacture, pre-launch, launch, and space operation, all have their own distinctive features. Although a space vehicle spends the majority of its life in space, it is evident that it must survive the other environments for complete success. In the following, we will not identify the manufacturing phase. However, it has an effect upon the reliability and the ability to meet design goals.

The next sections will address the different environments encountered by the spacecraft. The analysis of these environments will allow us to define rules and procedures to verify a certain TRL level of the satellite's components. These procedures will be presented in the next chapter.

3.1. Pre-launch Phase Environment

As stated before, the pre-launch environment should be studied to prevent damage on the spacecraft. The design, manufacture and assembly of a satellite, and its final integration into a launch vehicle are a long process. The different satellite components and subsystems may be stored for a considerable period of time prior to launch. Critical components that must be conserved in peculiar conditions, such as a given humidity or temperature, special care should be considered. To prevent this, control environments during such periods should be done to guarantee the perfect quality of the component in order to avoid failures on orbit.

3.2. Launch Phase Environment

The launch phase is very unpleasant for the entire payload, whether it is primary or secondary in terms of piggyback. This phase contemplates the change of environments, from the Earth environment to outer space environment. It is a sudden environmental change in a very short period of time. Summarizing, this

phase entails high levels of vibration, associated both with noise field and structural vibration, high levels of acceleration during ascent, mechanical shock due to pyrotechnic device operation and stage separation, a thermal environment that differs from Earth and a rapidly declining pressure. Besides, components must be electromagnetically compatible with other rocket's subsystems. These features are described separately below.

3.2.1. Acoustic Vibration Environment

The *acoustic vibration environment* is due to both launch vehicle's engines and also the aerodynamic buffeting as the vehicle rises through the lower region of the Earth's atmosphere. There are basically two main phenomena that turn into two acoustic/vibration peaks. The first one occurs at the moment of lift-off. When the rocket motor is fired, the exhaust produces a reflection at the ground that reaches the launcher. Also the overall rocket motor itself contributes to the peak by means of excitation of the structure produced by mechanical components, such as liquid fuel turbopump. The second peak happens when the rocket reaches the transonic flight. The launch nose is excited by the unsteady flow filed around it.

3.2.2. Launch Acceleration

The steady component of *launch acceleration* must achieve a speed increase of the order of 9 km/s. However, this value is rocker dependent. Generally, low mass vehicles produce higher accelerations whereas large mass vehicles (those carrying large payload or crew) experience lower accelerations. For multi-stage vehicles, the acceleration increases during the burn of each stage and peaks at stage separation.

3.2.3. Mechanical Shock

The *mechanical shock* is experienced when devices such as explosive bolts are used, or at ignition of rocker motor stage and their separation, launch vehicle or payload separation. These instantaneous events can provide extremely high-acceleration levels lasting only a few milliseconds locally. The accelerations are in the range of 2000 g to 3500 g depending on the launch system.

3.2.4. Thermal Environment

The *thermal environment* is determined by the temperature achieved at shroud during launch. This temperature arises from the aerodynamic friction forces of the vehicle moving at high velocity through the atmosphere. The temperature reached is determined by the specific heat of the shroud material and a balance between friction heating and radiative and convective heat loss.

3.2.5. Atmospheric Pressure

The *atmospheric pressure* declines during launch. The rate of the depressurization depends on the venting of the shroud volume. Venting control is important because of possible adverse static loads being placed on structural members.

3.2.6. Electromagnetic Interference

In order to ensure that *Electromagnetic Interference* (EMI) does not present a hazard, special care is required during payload integration. EMI may result in the activation of part of the payload, which could lead to catastrophically disasters and non-reparable spacecraft damage.

3.3. Space Phase Environment

The first problem encountered in the study of outer space environment is that of defining the different environments experienced. In order to reflect the fundamental differences in the nature of the local space environment, we will group space environment effects into five categories: *vacuum*, *neutral*, *plasma*, *radiation*, and *Micrometeoroid / Orbital Debris (MM/OD)*.

3.3.1. The Vacuum Environment

There are some problems associated with the vacuum environment. As a first issue that we encounter, we have the decrease of the *pressure* in function of the altitude. There are also inconvenient due to *Ultraviolet Radiation (UV)* exposure. Besides, the possibility of *contamination* due to either thin molecular films or small particulates can also produce damage. Finally, without the presence of an atmosphere, the spacecraft has to cool itself through *radioactive processes*. Operate under these conditions places constraints upon structures, choices of materials, and thermal control. Chapter 5 will present with more detail information about vacuum environment.

3.3.2. The Neutral Environment

All interactions with the neutral atmosphere are dependent on the *atmospheric density*. As such, they are of greatest interest for the lowest orbits, where the density is greater than higher orbits. Therefore, for neutral environment *thermosphere* and *exosphere* Fig. 3.1 are of big concern.

Although it is far too tenuous to support human life, in LEO, the neutral atmosphere is of sufficient density to cause significant *aerodynamic drag force* by creating interactions with a spacecraft. We can define the drag force equation as

$$F = \frac{1}{2} \rho v^2 C_d A , \quad (3.1)$$

where, ρ is the material density, A is the area of the object normal to the flow, and, C_d is the drag coefficient. To mitigate drag effects it would be necessary to create a low cross-sectional area perpendicular to the velocity direction. Besides, it would be necessary to orient sensitive surfaces and optical sensors away from the face that intercepts the atmospheric flux.

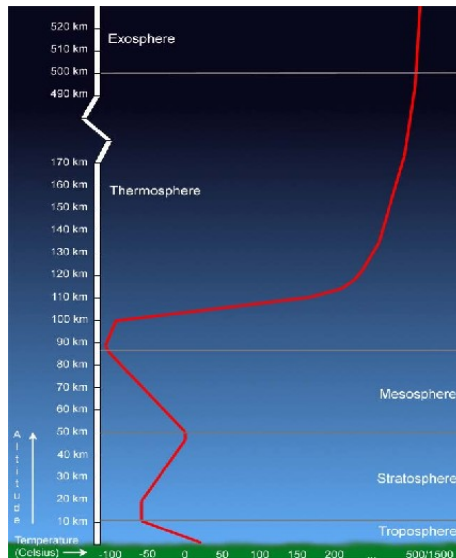


Fig. 3.1 The different layers of the atmosphere.

Moreover, the most abundant element in LEO is *Atomic Oxygen* (AO), which due to its highly reactive nature, may chemically erode surfaces or give rise to a visible *glow* that could interfere with remote sensing observations. AO interacts with a wide variety of materials, leading to oxidation or erosion and, generally speaking, degradation of materials' properties. As a result of that, AO is important for long-term missions. Another important effect is *glow*. In physics, glow, is defined as the light emitted by a substance or object at a high temperature without creating a flame. Glow may increase in brightness toward the red, peaking at about 6800 Armstrongs. Also, its intensity varies from material to material. To mitigate AO and glow effects it is necessary to choose materials that are resistant to AO and do not glow brightly. Nevertheless, experience indicates that materials that are not susceptible to glow are susceptible to atomic oxygen and vice versa.

3.3.3. The Plasma Environment

Plasma is produced when some atomic electrons receive enough energy to escape the electrical attraction of the nucleus. The result is a mixture of negatively charged electrons and positively charged atoms, which are called *ions*. More formally plasma can be defined as a gas of electrically charged particles in which the potential energy of attraction between a typical particle and its nearest neighbor is smaller than its kinetic energy.

A spacecraft that is subjected to plasma may be charged to high electrical potentials. This is of concern due to the possibility of *physical damage*, which could permanently damage spacecraft subsystems, or to create EMI, which could interfere with sensitive electronics. Moreover, plasma can cause other effects such as *noise* affecting the electronics and *errors* in the communications. The principal solution to mitigate these effects is to make the exterior surfaces uniform by shielding. Therefore, the conductivity would not be possible. In LEO, the solar UV ionizes the ambient oxygen and nitrogen atoms, producing plasma. Because photo-ionization is the dominant mechanism, this region is often referred to as the ionosphere. The plasma density is seen to vary both with local time and with solar cycle as indicated in Fig. 3.2.

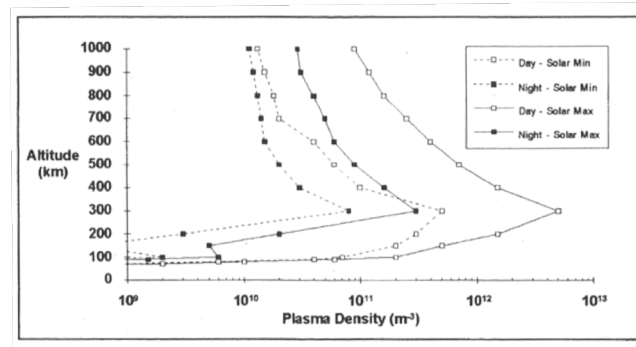


Fig. 3.2 The LEO plasma density as a function of altitude.

At low altitudes the percentage of ions is very small, approximately 0.1%, but the ionization approaches 100% when we move beyond LEO. Above LEO the ionized constituents are dominant over the neutrals (neutrals are defined as the common state of the matter, that means with no ionization) and this region is termed the magnetosphere.

In LEO ionospheric plasma has low energy but high density. Due to this fact, plasma cannot charge objects to high potentials but can supply high currents. In contrast, in Geostationary Earth Orbit (GEO), magnetospheric plasma has high energy but low density. Therefore plasma can charge objects to high potentials, but only low-charging currents are available.

As we mentioned before, the colder plasma found at lower altitudes is incapable of inducing significant charging. However, energetic particles are constrained to move along the magnetic field lines. As a result, spacecraft in low-altitude, high-inclination orbits may encounter the more energetic plasma that originates at higher altitudes and follows the magnetic field lines down to lower altitudes. Nevertheless, spacecraft will only pass through the polar region periodically during the course of its orbit and for a limited amount of time.

3.3.4. The Radiation Environment

In general, any energetic particle (electrons, protons, neutrons, heavier ions) or photon (gamma rays, X rays) can be considered ionizing radiation. As radiation moves through matter it may displace and/or ionize the material along its path. Some examples of damage that radiation may produce to space systems are decreasing the power output of solar arrays, creating spurious signals in focal planes, or inducing single-event phenomena in spacecraft avionics.

Depending on the nature of the emitted radiation, three classes of radiation can be defined; *alpha*, *beta* and *gamma*. Alpha particles are helium nuclei, beta particles are either electrons or positrons, and gamma rays are energetic photons.

Photons can alter the material properties. They are unaffected by electrostatic forces, they will move in straight lines until they undergo an interaction with the target material. The probability of intersection is the total cross section. Normally,

charged particles will be stopped by a finite amount of shielding, while photons follow an exponential decay. For photons, shielding will reduce the flux but will not stop all the particles; therefore we can talk of a penetration depth.

Besides, there are also three naturally occurring sources of radiation in space: the *Solar Energetic Particles* (SEPs), the trapped radiation belts or *Van Allen belts*, in honor of the principal investigator who discovered them, and finally, *Galactic Cosmic Rays* (GCRs).

During coronal mass ejections the Sun ejects significant amounts of alpha particles, electrons, a few heavier ions, and protons (which are the dominant constituents). These particles are called *SEPs*. They are modulated by solar storms and solar 11-year cycle (which has 7 years of solar maximum, and 4 years during solar minimum). Large solar particle events and trapped electron fluxes in the belts are known to occur with greater frequency during the declining phase of solar maximum. Contrariwise, trapped proton fluxes in LEO reach their maximum during solar minimum. SEP show a wide range of distributions in outer space. It should be noted that while the dose due to large SEPs may be quite high in some orbits, the Earth's magnetic field (magnetosphere) provides a great deal of shielding.

The *Earth's magnetosphere* consists of both an external and an internal magnetic field. The external field is the result of the solar wind. The internal or geomagnetic field originates primarily from within the Earth and is approximately a dipole field at low altitude, see Fig. 3.3. Although the Earth magnetic field is a very efficient shielding for satellites, it also produces the *Van Allen belts*. They are very influential in satellite mission design due to the pass through them can cause upsets and important damages to satellites. Moreover, at lower altitudes, an additional issue of the Van Allen belts is due to the depression in the magnetic field caused by the difference between the magnetic and geographic axes. This fact creates an anomaly called the *South Atlantic Anomaly* (SAA). For many LEO satellites, the upsets due to protons in the SAA are of a big concern.

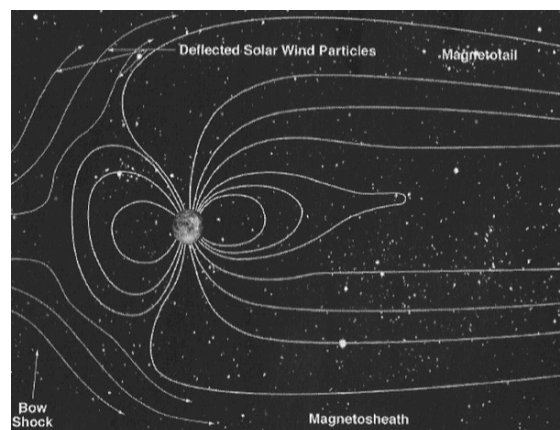


Fig 3.3 The Earth's magnetosphere.

Apart from the Van Allen belts and the SEP there are other energetic particles that can affect our spacecraft, the *GCR*. These are more energetic than particles belonging to Van Allen belts. GCRs are energetic nuclei, mostly protons, originated outside the solar system. Galactic cosmic radiation consists of an isotropic,

energetic and a low flux of particles, approximately $4 \text{ particles/cm}^2\text{s}$ of $10^8\text{-}10^{19} \text{ eV}$. Like the SEP and the Van Allen trapped particles, the GCR flux is also dependent on the solar cycle, being the GCR rate highest during solar minimum, see Fig. 3.4.

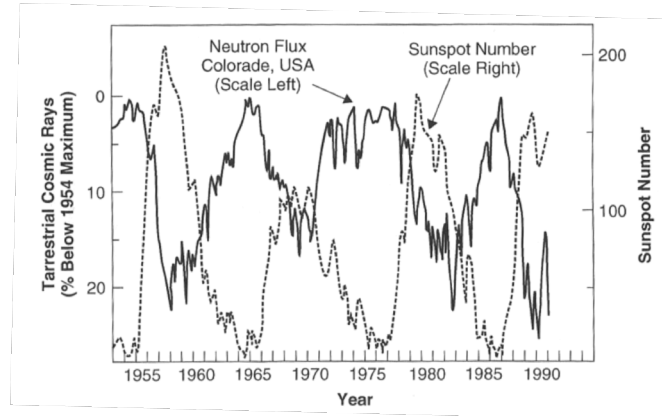


Fig 3.4 Variation in cosmic rays due to the solar cycle.

During spacecraft design it is necessary to have a good understanding of the radiation dose that will be received by the electronic elements to be able to apply the correct mitigation techniques. For example, it is important to notice if certain electronic part cease to function after exposition to the radiation dose expected. If this occurs, additional shielding may be required to reduce the radiation dose, or, otherwise, it may be necessary to find other electronic parts that can tolerate the dose. Moreover, it is necessary to study the exactly radiation environment where the satellite will be placed because an effective shielding depends on it. For example, for charged particles or photons the key is to get mass, therefore high-density materials work best. On the other hand, for neutrons, low-density materials shields are the best. Finally, another important mitigation technic is to design the spacecraft with more redundancy and to install software capable of recovering the system from latchups and upsets.

3.3.5. The MM/OD

On clear nights, it is usual for a star-gazer to witness the right trails of a handful of shooting stars every hour. These shooting stars are actually tiny pieces of matter that burn up upon entering the Earth's atmosphere. Our solar system comes with its own naturally occurring background of dust that results from the breakup of comets, asteroids, and so on. These naturally background particles are called *MM*. The *MM* flux is not constant, but varies slightly over the course of the year during events known as meteor showers. These are times when the Earth's orbit intersects the orbital path of the cloud of dust. They generally have velocities of around 17 km/s.

On the other hand, the artificial environment formed by pieces of non-operational spacecraft, such as, boost stages or solid rocket fuel particulates are referred to as *OD*. They are mostly quite small less than 1 cm, but only those object greater than 10 cm are tracked routinely. Nevertheless, all of them are of great concern because of their large kinetic energies. Artificial *OD* are found in orbit around the Earth with velocities on the order of 8 km/s. It is easy to see that *OD* collision will occur mainly

on ram-facing surfaces (object's face perpendicular with the current flux). Unlike MM, the OD flux is affected by the solar cycle (via aerodynamic drag). It is a big concern that the mass of OD continues to grow as the satellite population increases at the rate of about 230 trackable objects per year. Due to the OD flux is closely tied to spacecraft launches, the most popular altitudes and inclinations are where the largest problems are expected.

The primary cause of concern from both MM and OD is physical damage upon impact. Some examples are the erosion of materials surface, changes in thermal control properties, the liberation of particles or the generation EMI. In manned missions, where the cabin must be pressurized at a certain level, the damage produced by an impact of an MM/OD is of great concern. The hole produced by the MM/OD can depressurize the cabin, making also an easy way of entering for plasma and AO. It is possible to mitigate or decrease MM/OD effects by pointing sensitive surfaces away from ram, flying at altitudes and inclinations where debris are minimized, as well as utilize leading edge bumper shield to protect critical components.

CHAPTER 4. PROCEDURES AND MECHANISMS TO QUALIFY COMPONENTS FOR SPACE TECHNOLOGY

In the previous chapter we presented the issues regarding the space environment effects. They were addressed to better understand which are the implications for spacecraft design during all the mission phases. We saw that different effects arise in those phases that could completely destroy a given component making the whole mission fail.

In principle, any component or subsystem can be put on orbit as there does not exist any legal or design constraint. However, the cost associated with a mission is extremely high (of the order of millions of dollars depending on the mission goals and requirements) and contractors only rely on components that will survive all the phases without being damaged. It's because of that that some procedures and mechanisms are needed to qualify components for space missions.

Through the history, there have been some events and programs to come up with common space environments standards. For instance, in 1990s the National Science Foundation (NSF) formed the Space Weather program that aimed to the development to predict changes in the space environment. The European Space Agency (ESA) has also a similar program. The International Standards Organization (ISO) did also form a space systems technical committee in 1990s that is working to develop internationally recognized space environment standards.

The common objectives of these organizations are to predict and to avoid spacecraft subsystems degradation and to find the relationships between the space environment and spacecraft, or space instrument, operating principle, and design alternatives. However, they did not clearly define a metric to support the evaluation of the maturity of a given technology. In 1974 National Aeronautics and Space Administration (NASA) originated the TRL methodology. During the 80s, they published several articles on reusable launch vehicles utilizing the TRL methodology. These documented an expanded version of the methodology that included design tools, test facilities, and manufacturing readiness. It was not until 1989 when NASA provided a first definition of the TRL procedures based on a 7 level structure. The levels were defined as

1. Basic principles observed and reported.
2. Potential application validated.
3. Proof-of-concept demonstrated analytically and/or experimentally.
4. Component and/or breadboard laboratory validated.
5. Component and/or breadboard validated in simulated or real space environment.
6. System adequacy validated in simulated environment.
7. System adequacy validated in space.

Currently, different definitions are used by different agencies, even though they are somewhat similar. The most common definitions are those used by the Department of Defense of the USA and the NASA. Nevertheless, the ESA has already defined

its own TRL procedures and they are becoming more popular and followed by European companies above all.

In the next section we will present the details of the TRL described by the ESA since they are the procedures that will be used along the work [1]. Then, we will explain the procedures to obtain a certain TRL. Finally, we will present which are the experiments and simulations that have been chosen such that the microprocessor achieves a certain TRL level. The theoretical aspects of the experiments and the results are to be presented in future chapters.

4.1. Technology Readiness Level

TRLs are a set of management metrics that enable the assessment of the maturity of a particular technology and the consistent comparison of maturity between different types of technology, all in the context of a specific system, application and operational environment. TRL are applicable to hardware and software components. However, they follow different guidelines for the definition of TRLs. In the following, we will only present the TRL definitions of hardware since no software is analyzed in this thesis. For further information, the reader is referred to [1].

Table 4.1 provides the complete set of basic definitions and explanations of the TRLs applicable to hardware.

Table 4.1 The basic technology readiness levels.

Readiness Level	Definition	Explanation
TRL 1	Basic principles observed and reported	Lowest level of technology readiness. Scientific research begins to be translated into applied research and development.
TRL 2	Technology concept and/or application formulated	Once basic principles are observed, practical applications can be invented and Research and Development (R&D) started. Applications are speculative and may be unproven.
TRL 3	Analytical and experimental critical function and/or characteristic proof-of-concept	Active research and development is initiated, including analytical / laboratory studies to validate predictions regarding the technology.
TRL 4	Component and/or breadboard validation in relevant environment	Basic technological components are integrated to establish that they will work together.
TRL 5	Component and/or breadboard validation in relevant environment	The basic technological components are integrated with reasonably realistic supporting elements so it can be tested in a simulated environment.
TRL 6	System/subsystem model or prototype demonstration in a relevant environment (ground or space)	A representative model or prototype system is tested in a relevant environment.

TRL 7	System prototype demonstration in a space environment	A prototype system that is near, or at, the planned operational system.
TRL 8	Actual system completed and "flight qualified" through test and demonstration (ground or space)	In an actual system, the technology has been proven to work in its final form and under expected conditions.
TRL 9	Actual system "flight proven" through successful mission operations	The system incorporating the new technology in its final form has been used under actual mission conditions

The nine TRLs followed by ESA were mentioned before. However, for a complete definition of the technologies readiness assessments (to be presented in the next section), a more detailed explanation of the TRLs is needed. The paragraphs that follow provide clear definitions regarding each of the nine technology readiness levels.

TRL 1

TRL 1 occurs at the end of scientific research and the beginnings of technology development; it is lowest level of technology maturation, just beyond basic science, at which an assessment of technology readiness might be performed. At this level, basic scientific research has resulted in the observation and reporting of basic principles and these begin to be translated into more applied research and development. Examples of TRL 1 might include studies of basic properties of materials (e.g., tensile strength as a function of temperature for a new fiber).

TRL 2

Once basic physical principles are observed, practical applications of those characteristics can be identified. This step in the maturation of a new technology is TRL 2: the creation of a new concept based on a new or existing physical or mathematical principle. At TRL 2, prospective system applications are still rather speculative. At this point, there is no specific experimental proof or detailed analysis to support the conjecture. However, it is still necessary that the new technology or concept should be described in sufficient, internally consistent detail such that anyone skilled in the field can understand it, and evaluate its potential usefulness.

TRL 3

At this step in the technology maturation process, active R&D is initiated. This must include both analytical studies to set the technology into an appropriate context and laboratory based research or tests to physically validate that the analytical predictions are correct. These studies and experiments should constitute "proof-of-concept" validation of the applications/concepts formulated at TRL 2. TRL 3 includes both analytical and experimental approaches to proving a particular concept. Which approach is appropriate depends in part on the physical phenomena involved in the invention. For example, new algorithms or computational techniques may be proven analytically. However, other inventions will require physical experimental validation.

TRL 4

Following successful proof-of-concept testing for critical functions or characteristics, the basic technological elements involved in an invention must be integrated to establish that the pieces will work together to achieve concept-enabling levels of performance at the level of a component and/or breadboard. This validation at TRL 4 must be devised to best support the concept that was formulated earlier, and should also be consistent with the requirements of potential system applications. However, validation at this level is relatively low-fidelity compared to the eventual system applications.

TRL 5

TRL 5 requires the validation of a component and/or breadboard in a relevant environment (i.e., one that represents the expected operational environment in critical aspects). This means that the basic technological elements must be integrated with reasonably realistic supporting elements so that the total application (e.g., at the component-level, sub-system level, and/or system-level) can be tested in a simulated or somewhat realistic environment. Anywhere from one to several new technologies might be involved in the demonstration. In other words, at this stage, the fidelity of the component and/or breadboard being tested has to increase significantly beyond those that were demonstrated at TRL 4 or lower.

TRL 6

A major step in the level of integration and/or fidelity of the technology demonstration follows the completion of TRL 5. At TRL 6, a representative model or prototype system or system, which would go well beyond an ad hoc discrete component level breadboard, must be tested in a relevant environment. It is important to note that although reaching TRL 6 does not generally require flight of a complete system in space, if the only relevant environment is the environment of space, then the system model/prototype must be demonstrated in space.

TRL 7

TRL 7 is a significant but optional maturation step beyond TRL 6, requiring an actual system prototype demonstration in the expected operational environment (e.g., in space in the case of space applications). Typically, a TRL 7 demonstration is only implemented in cases of high technical risk and/or when systems-level innovation is necessary to achieve mission goals and objectives. In the event that a TRL 7 demonstration is called for, the prototype should be near or at the scale of the planned operational system and the demonstration must take place in the actual expected operational environment. The driving purpose for achieving this level of maturity must be tied to assuring system engineering and development management confidence.

TRL 8

By definition, all technologies being applied in actual systems go through TRL 8. In almost all cases, this level is the end of true system development for most technology elements. In the case of a space transportation system being developed, for example, TRL 8 could comprise the completion of Design,

Development, Test and Evaluation (DDT&E) through theoretical first unit for a new type of vehicle. TRL 8 could also often also involve cases in which a new technology is being manufactured and integrated into an existing system. Alternatively, TRL 8 might also involve developing, loading, testing and deploying for operations successfully some new software involving a revised approach to control algorithms in a spacecraft while it is in orbit.

TRL 9

TRL 9 is the level of maturity reached by a new system when it is launched and operated successfully (together with all of its constituent technologies). Typically, this level of maturation requires that the system be operated in the originally planned environment, and with performance characteristics that satisfy the requirements of the system and the mission. The key distinction between TRL 8 and TRL 9 is the final step of launch and operations.

4.2. Technology Readiness Assessments

This section provides a standard set of guidelines for the use of TRLs in conducting Technology Readiness Assessments (TRAs). Typical processes for conducting TRAs are described. For a set of detailed guidelines for TRAs for the different TRLs, the reader is referred to [1].

There are several general steps that must be accomplished in the process for conducting an effective TRA. These include:

- Formal definition of the terms of reference for the assessment.
- Identification of key supporting data.
- Identification of TRA participants.
- Development and delivery of technology data to the TRA.
- Implementation of the TRA itself.
- Development of a TRA report.

A set of criteria must be used to determine whether a new technology has satisfied the various aspects of the maturation that define a TRL. As a consequence, a given TRL is said to be achieved if and only if all of the criteria are satisfied and not before.

In order to conduct a technology readiness assessment at any TRL level, the same types of information should be examined to determine that a given TRL has been achieved. Fig. 4.1 depicts a generic flow diagram for a TRA, including four principal areas for TRL criteria.

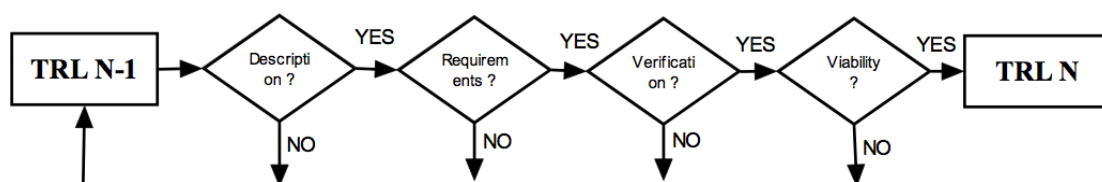


Fig. 4.1 Generic TRA steps.

As it can be seen from the figure, there are four areas: *description*, *requirements*, *verification*, and *viability*. Description refers to the details of the research and development that has been performed, or the technology that has been advanced. The requirements involve the degree to which a future application of a technology is known. The characteristics of the application must be well defined to be able to judge whether a new technology will be able to meet those requirements. Verification measures the degree of similarity of the testing environment and the environment in which the technology will be used in operations. It also measures the degree of performance level that the technology has achieved in the needed environment. Finally, the viability step faces the issue of establishing both technical risk and programmatic viability effort. It is important to know if a given technology can be further developed and, if so, with what technical risk and effort.

Additionally to the previously proposed areas, time should also be considered (in connection with technology evaluation). If the technology was developed in the past, and it needs to be reused or reevaluated today, particular attention should be paid to the possible obsolescence of the technology.

If more than one technology that are intended to work together must be evaluated, it is better to evaluate them separately, and then associate to them two TRL values, namely, the average and the lowest.

Depending on the level of maturity of the technology, the participants that validate the results must be different. Besides, independent review takes more importance as the maturation evolves. In particular, as the degree of integration of individual technologies increases and the testing environment more closely approaches the planned operating environment, the role of prospective customer organizations should increase. Table 4.2 shows a summary of the validation processes and independent reviews.

Table 4.2 Summary of independent review and validation processes.

TRL Levels	TRA Independent review and validation participants
TRL 1-3	The technologists involved in the conduct of the R&D should lead Review and Validation of TRA results. However, even at this level a TRA should involve the participation of the management of the technology development organization.
TRL 4	Independent Review and Validation of TRA results should be led by management of the technology organization, with the participation of both the technologists involved and the leadership of prospective system organizations.
TRL 5	Independent Review and Validation of TRA results should be led cooperatively by the management of the organization responsible for development of the technology and by that of the prospective system application of the new technologies being developed. Technologists and participants in the system development project should play significant roles in the conduct of such reviews.

TRL 6-9	Independent Review and Validation of TRA results should be led by the management of the organization responsible for development of the prospective system application of the new technologies under development (or operation for TRL 9). Technologists and participants in the system development project should play significant roles in the conduct of such reviews.
---------	---

4.3. Conducted Experiments

In the previous sections we have presented the mechanisms and procedures needed to space-qualify a certain component. As it was stated before, the objective of this project is to make some laboratory experiments and simulations on the microprocessor to achieve, or to partially achieve the TRL level 3. TRL level 1 and level two were exposed in Chapters 1 and 2. Basic definition of the microprocessor and its specific potential space applications were described in those chapters.

In this section, we show what experiments are of interest and why. Then, the conducted experiments will be exposed in Chapter 6.

Chapters 3 presented all the physical phenomena associated with all the different mission phases, that is, pre-launch, launch, and space operation. Recall that depending on the phase the component is, it has to deal with specific environmental issues. For example, increase of shroud temperature was produced due to atmospheric drag. However, not all the effects affect directly the microprocessor. Considering the launch phase, the acoustic vibration environment does not apply directly to the microprocessor, since the subsystem to deal with these effects is the structure of the satellite. We assume, therefore, that the structure is well designed according to the launcher specifications so that it fully resists the vibration spectrum. For the same reason, mechanical shock and launch acceleration are out of interest. Since the experiments are only conducted to the microprocessor without integration of other components, the EMI analysis is also not considered. Hence, the only effects of interest produced during launch phase are thermal and pressure effects (in fact these two are related as it will be shown later).

On the other hand, the operation phase also presents some non-applicable effects. Notice that the microprocessor is a central component of the satellite, so it is not exposed to certain environmental conditions. Moreover, the satellite has some sort of basic shielding that protects it in front of some of these effects. For example, the solar UV, glow, and AO are effects that directly apply on the satellite surface. Thus, the surface must be designed with proper materials to resist the effects of these phenomena explained in Chapter 3. Additionally, impacts of MM/OD and drag effects should be handled by the geometry and hardness of the structure. As a result, radiation environment and temperature and pressure effects of the vacuum environment will be analyzed.

The proposed experiments and simulations to be done will be based on the three potential influences presented before: thermal, pressure and radiation effects. The justification proceeds in the following paragraphs.

For the case of the processor used in the WikiSat, i.e., the ATmega 168 [2], the manufacture says that the operating temperature range is between -40°C to 85°C (measured taken at sea level ambient conditions). Between this range of temperatures the processor will always work showing good performance. Nevertheless, it may also survive to a higher or lower peak of temperature than the operating range, but only for short periods of time. A continuous exposition to temperatures outside the range could yield to non-reparable damage on the microprocessor. In low-cost platforms with only one central processor unit, it should be avoided to expose the component at these temperatures; otherwise we could jeopardize the whole mission.

It is clear that these commercial components are designed exclusively for Earth purposes. It is not common to exceed the temperature values presented before in normal conditions close to sea level. However, as it was shown in Chapter 3, the temperature of the shroud at launching may increase considerably due to different phenomena. Moreover, when any celestial body eclipses the satellite the sunlight does not reach it making its temperature decrease to very low values. On the other hand, if it is in direct visual contact with the Sun, it experiences periods of very high temperatures (on the order of 80°C - 150°C depending on the orbit and on the optical properties of the satellite surfaces).

The low pressures experienced during launch and at outer space do not present a problem to the proper function of the microprocessor. Nevertheless, thermal convection is not produced in low-pressure environments. This, indeed, presents a problem. If no convection is possible, the local temperature is increased, and that translates into a higher internal temperature experienced by the microprocessor. As a consequence, the maximum operating temperature is realized more easily in space than on the ground. The experiment to be conducted will expose the microprocessor to a vacuum environment with a varying temperature.

Extreme radiation is only experienced in outer space, besides some very definite environments on the Earth. It must be analyzed since the structure of the satellite is not able to protect the inside from it, as the radiation is composed by very high energy particles and often with high atomic mass. These energetic particles are very difficult to protect from, and shielding materials may be needed in some cases to guarantee the survivability of the component. The conclusions of these effects will be presented with simulations, since no experiment was conducted. Besides, it is sometimes difficult to evaluate the effects of some particular radiation in the laboratory, such as for example GCR, and the only way to learn the behavior of the component is by real exposure of it in outer space.

CHAPTER 5. SPACE TECHNOLOGY QUALIFICATION: THEORETICAL BACKGROUND

In this chapter we present the theoretical concepts concerning two experiments to be done to space-qualify the microprocessor. As stated in the previous chapter, only three experiments will be performed to obtain conclusions about the survivability of the given processor. However, only the vacuum environment and the radiation analysis may need a theoretical background to better understand the experiments presented in the next chapter [6,9]. The chapter is organized as follows. The vacuum environment is firstly addressed, presenting with detail the effects on the pressure, the solar UV, the molecular contamination, and finally the particulate contamination. Then, the radiation effects are studied. Total Dose (TD) effects are presented and its two categories, Total Ionizing Dose (TID) and Single Event Effects (SEE) are deeply analyzed. These are the most harmful, and thus, they will be exposed in more depth.

5.1. Vacuum Exposure Analysis

At 100 km altitude the ambient atmospheric pressure is over six orders of magnitude less than that found at sea level. Moreover, our atmosphere absorbs the solar UV, therefore, spacecraft in orbit must deal with its effects. A third big concern is the possibility of contamination due to either thin molecular films or small particles.

5.1.1. Pressure

The *pressure* in the Von Kármán line (marking the legal frontier of space) is reduced by six orders of magnitude as it is shown in Fig. 5.1. Thus, relatively compared with Earth pressure, space environment can be assumed to be vacuum.

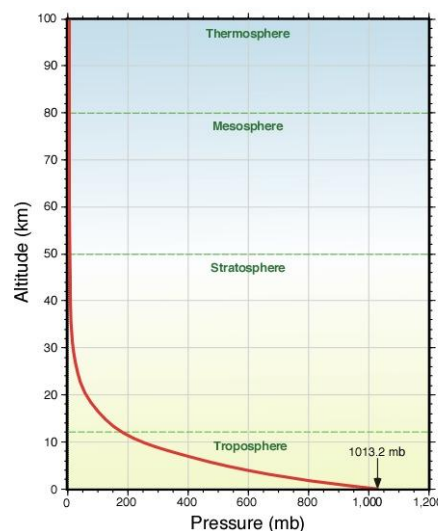


Fig. 5.1 Atmospheric pressure versus altitude.

If there is crew in the space vehicle, it has to be hermetically sealed to make sure that the pressure is suitable for humans. Hence, it is necessary to take into account the forces that the satellite structure will have to withstand due to the differences between internal and external pressure and the possibility of depressurization because of MM/OD impacts. However, if the space vehicle is not manned, vents can be placed in it to allow the internal atmosphere to escape from the satellite during launch.

5.1.2. Solar UV

Another important matter is *Solar UV* exposure. As depicted in Fig.5.2, the Earth's ozone layer absorbs most of the Solar UV making the Earth a habitable place. Nevertheless, satellites have to deal with UV effects, since they are placed above of the ozone layer.

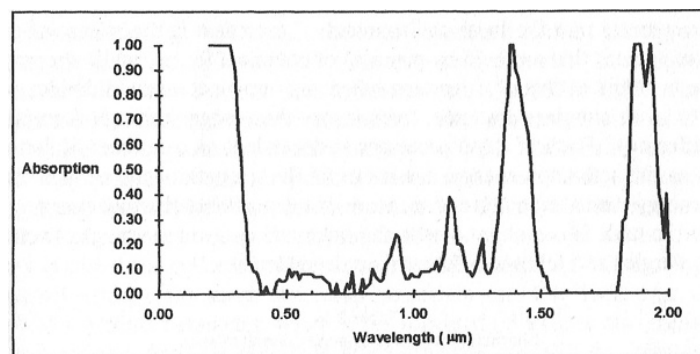


Fig. 5.2 Atmospheric absorption.

UV radiation is energetic enough to break molecular bounds, which degrades material properties. As a result, the physical characteristics of many materials change upon exposure to UV radiation. The energy of a single photon is related to its wavelength λ , or frequency ν , according to the following relation:

$$E = h\nu = \frac{hc}{\lambda}, \quad (5.1)$$

where, h is the Planck's constant and c is the speed of light. From Eq. (5.1) we are able to conclude that, since UV has a very short λ it is capable of changing physical characteristics of many materials by means of breaking materials chemical bonds.

5.1.3. Molecular Contamination

The spacecraft itself is a source of contamination during launch or on orbit operations, due to basically its own propulsion system. As a consequence of contamination ambient pressure, *molecular contamination* may occur through a process called outgassing. The satellite will contain fractional amounts of "volatile" chemicals, basically on the surface. These chemicals migrate from the surface and escape into the local atmosphere, which may randomly impact other surfaces from the satellite. If these outgassed particles were to build up on a thermal control surface or on sensitive optics, the resulting properties could be severely degraded.

However, increasing surface temperature considerably decreases the residence time of the particles on it.

Outgassing depends on a number of different processes: diffusion, desorption and decomposition. Diffusion is the homogenization that occurs from random thermal motion. Desorption is defined as the release of surface molecules that are held by physical or chemical forces and decomposition is a type of chemical reaction where a complex compound divides into two or more simpler substances.

The contaminant molecule will remain attached to the surface until, following the random probabilities of quantum mechanics, it acquires enough energy to escape the electrical attraction to the surface. The average residence time on the surface is therefore related to the surface temperature and is approximated by:

$$\tau(T) = \tau_0 e^{E_a/RT}, \quad (5.2)$$

where, τ is the residence time measured in seconds, τ_0 is the residence time at 273.15 K, also measured in seconds. E_a is the activation energy for desorption of contaminant measured in $J/mole$. R is the universal gas constant in $J/mole \cdot K$. Finally, T is the temperature measured in K .

As we can see from Fig. 5.3, an increase of the surface temperature yields to smaller residence time.

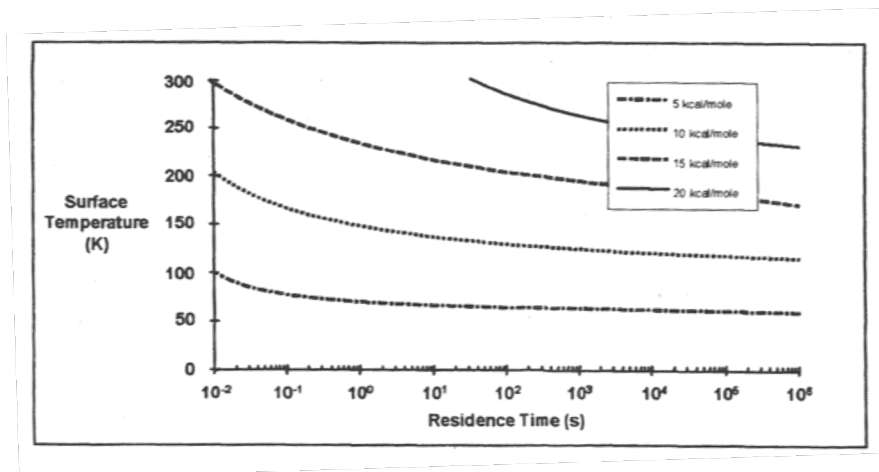


Fig. 5.3 Residence time of contaminants.

5.1.4. Particulate Contamination

Another kind of contamination is *particulate contamination*. It refers to the micron sized pieces of matter that inevitably builds up on exposed surfaces during manufacturing and processing. Therefore, particulate contamination is generally deposited during manufacturing, test, or launch and not during on-orbit operations. These particulates are directly related to air quality, (amount of particulates in the surrounding air) on ground operations and, not to the space environment. The only real concern for particulate contamination is for optical sensors.

The buildup of particulates on a surface is directly related to the amount of particulates in the surrounding air. In SI units, the name of the air class is taken

form the base 10 logarithm of the maximum allowable number of particles, 0.5 μm and larger, per cubic meter.

$$\text{particles}/\text{m}^3 = 10^M \left(\frac{0.5}{d} \right)^{2.2}, \quad (5.3)$$

where, M is the numerical designation of the class in SI units and d is the particle size measured in μm .

For example, cleanrooms, typical of most spacecraft manufacturing rooms, have a class M 5.5. On the other hand common industries have an air class M 8.

The total number of particles deposited on a surface as a function of time is given by:

$$n(t) = t \cdot p \cdot N_c^{0.773}, \quad (5.4)$$

where, p is a normalization constant, N_c is the numerical designation of the class in English units, and t is the time measured in seconds.

Particulate contamination changes the characteristics of the underlying surface. It is straightforward to verify that an obscuration level great enough to significantly impact a thermal control radiator or a solar array could easily be detected, and eliminated by means of cleaning before launch.

Particulates are deposited on surfaces during ground operations. However, these particulates may be released on orbit by nominal spacecraft operations. On unmanned spacecraft this may occur due to articulation of solar arrays, thermal expansion/contraction, the release of covers, etc. On manned missions, venting and water dumps may generate particulates.

5.2. Radiation Exposure Analysis

In this section we present a more accurate description of the radiation environment and its effects on the electronics.

5.2.1. TD Effects in Aerospace

There are two different ways in which radiation can cause effects on spacecraft. These are *TD* effects and *Displacement Damage* (DD).

On one hand, *TD* effects are the amount of energy deposited in a material. Mostly due to electrons and protons. TD effects can result in device failure or biological damage to astronauts. It can be measured in terms of the absorbed dose, which is a measure of the energy absorbed by matter. Absorbed dose is quantified using either a unit called the rad (an acronym for *radiation absorbed dose*) or the SI unit, which is the *Sievert* (Sv).

When radiation interacts with an atomic electron the most likely effect is that the atom becomes ionized. Because energy is conserved, any energy lost by radiation would be transferred to the atomic electron. Ionizations have the result of moving charge carriers, effectively increasing the conductance of the material. This may allow small leakage currents to flow in dielectrics. Although this sounds fairly benign, it can lead to long-term consequences, especially in silicon dioxide, which

is a key component in many devices. Electron-hole pairs that are created by ionizations recombine and drift under the influence of any internal electric fields. Traps make it more difficult for subsequent majority carriers to travel, thus further decreasing current flow.

TD effects are also divided in two different subcategories, TID and SEE. Since both TID and SEE arise from ionizing radiation, it is important to address the difference between the two with respect to design and analysis. TID is defined as a long-term failure mechanism meanwhile SEE is described as an instantaneous failure mechanism. Therefore, TID failure rate can be described as *Mean Time Between Failure* (MTBF), but SEE must be expressed in terms of a *random failure rate* [10].

On the other hand, the amount of radiation dose that results in displacement is called simply DD. DD is one of the causes of damage in avionics subsystem. If an atom acquires enough energy, it may break its bound to neighboring atoms and become physically displaced from its original location. It is much less likely than ionizing radiation, but it is of huge significance for electronic devices.

Displacements alter the structure of the atomic lattice, invariably making it less orderly. If the lattice structure is disturbed, the electronic properties of the device are altered. When an energetic particle collides with the nucleus of an atom in the target material, the nucleus in the target may be dislodged, or displaced, from its original location. The displacement creates a vacancy called interstitial. In many cases, the recoiling atoms have enough energy to create a cascade effect, resulting in many defect formed within a small area. When neutrons, protons, or heavy ions collide with a nucleus of an atom the energy may be absorbed by the nucleus itself. Some nuclear interaction may excite atomic nuclei. Excited nuclear states are unstable, and the nucleus will decay by emitting a gamma ray, which in turn may produce ionizations. If the nucleus of a target atom absorbs a neutron or proton, it will change into a different element, which will very likely be radioactively unstable. The unstable atom will then decay by emitting alpha, beta or gamma radiation. The decay by-products can in turn create additional ionizations or displacements.

DD usually occurs only if the radiation source is an energetic neutron, proton, or heavy ion. Therefore, electron radiation, which is half of the natural space radiation environment, does not produce displacements.

All charged particles will interact effectively with atomic electrons. Similarly, all charged particles can, in principle, interact with the nucleus. However, because the nucleus of most atoms is much more massive than electrons, electron radiation does not effectively cause displacement damage. Low-energy protons would also have a hard time creating displacements. However, as the proton energy increases, the possibility of displacement damage increases. Heavier ions, being more energetic are more effective at creating displacements. Photons, having no electrical charge, will interact indirectly with both the electrons and nucleus. Therefore, their main effect is to create ionizations.

Finally, neutrons having no electrical charge will not interact effectively with the atomic electrons. They will travel relatively unimpeded until they approach a nucleus and nuclear forces become significant. They mainly induce displacement or other nuclear events.

5.2.2. TID

TD radiation, as it is mentioned before produces ionizations and atomic displacements. Total dose radiation then causes gradual global degradation of device parameters. It is necessary to overcome an ionization threshold to produce significant damage in the electronics.

The TID in LEO is obtained adding the contributions of trapped pond electrons of the Van Allen belts, of energetic particles produced by SPEs, and finally, of cosmic rays.

In Fig 5.4 we can see the annual dose of protons and electrons as function of orbital altitude. Besides altitude, annual dose also depends on the orbit orientation and time (due to solar 11-year solar cycle). Analyzing only LEO orbits, it is seen that the worst case of radiation due to protons occurs at 1.200-1.300 km. Meanwhile the electron peak fluency is situated at 1.200 km. However, if all the altitudes are taken into account, not only the LEO ones, the most important fluency of electrons occurs at 20.000 km. Moreover, due to protons only place altitudes from 1.000 to 10.000 km we can assume that they only affect satellites near the inner Van Allen belt. Therefore, TD in LEO is principally due to protons.

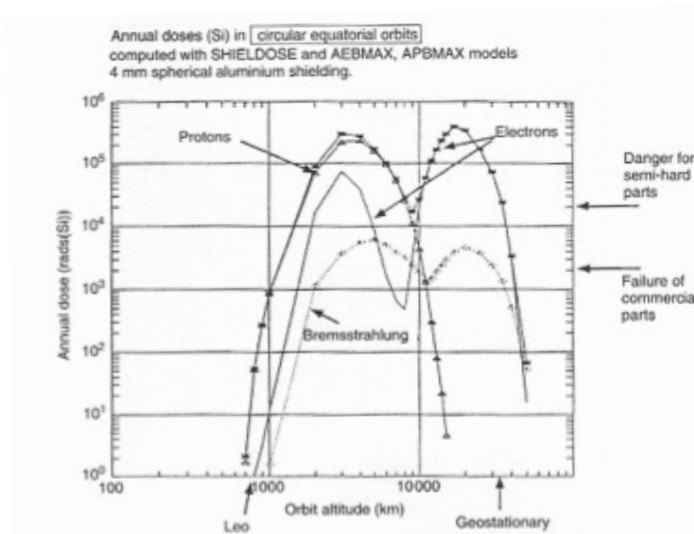


Fig. 5.4 Variation of the computed annual dose on circular orbits as a function of altitude.

Satellites and space probes typically encounter TID between 10 and 100 krad in Silicon. As TID increases, materials degradation increases, for example, solar cell output will decrease. Long-term exposure can cause device threshold shifts, increased device leakage and power consumption, timing changes, and decreased functionality. TID effects may be mitigated using radiation hardened devices and shielding. Electrons and low energy protons can be partially mitigated with shielding.

In semiconductors, the ionization excites carriers from the conduction to valence band. The ionizing radiation primarily affects gate and field oxide layer, SiO₂. Ionization produces electron-hole pairs. The electrons produced have high mobility

and are quickly swept away, but the holes have much lower mobility. Trapped charge, in the oxide and at interface regions, changes the threshold voltage and mobility of the gate and field-oxide transistors, thereby modifying their characteristics [12].

5.2.3. SEE

The most usual result that occurs when radiation impinges upon matter is ionization. As a result, ionizing radiation creates tiny spikes of electrical current. Cumulatively, these current spikes give rise of the total dose effects. Individually, they can give rise to a completely different category of phenomena. It would eventually be possible for the current spike produced by a single particle to interfere with the operation of many electrical devices. The resulting disruptions are called *SEE*. We can distinguish three main kinds of SEEs, *Single Event Upset* (SEU), *Single Event Latchup* (SEL), and *Single Event Burn-out* (SEB).

When considering SEU, the deposited charge must be sufficient to flip the value of a digital signal. SEU normally refers to bit flips in memory circuits (Random Access Memory (RAM), Latch, flip-flop) but may also in some rare cases directly affect digital signals in logic circuits. In any case, the deleterious effect is transient, and can (at least in principle) be detected and corrected by specialized error-correcting software or hardware (watchdog timers, for example).

On the other hand, SEL considers the effect created to the bulk of Complementary Metal-Oxide-Semiconductor (CMOS) transistors. Bulk CMOS technologies I (not Silicon On Insulator) have parasitic bipolar transistors that can be triggered by a locally deposited charge to generate a kind of short circuit between the power supply and ground. Complementary metal-oxide-semiconductor (CMOS) processes are made to prevent this to occur under normal operating conditions but a local charge deposition from a traversing particle may potentially trigger this effect. SEL may be limited to a small local region or may propagate to affect large parts of the chip. The large currents caused by this short circuit effect can permanently damage components if they are not externally protected against the large short circuit current and the related power dissipation.

Finally, SEB refers to destructive failures of power Metal Oxide Semiconductor Field Effect Transistor (MOSFET) transistors in high power applications. For HEP applications this destructive failure mechanism is normally associated to failures in the main switching transistors of switching mode power supplies.

Moreover, the characteristic of an individual ionizing particle are not known, so in these cases we discuss the total energy available to ionization from the nuclear reaction that led to the SEE. Therefore, we have two different ways to produce a SEE, by producing a single event interaction in a localized region of satellite's circuit that can lead to a seemingly spontaneous transient. And got the critical charge of TID.

The SEE community commonly uses two different ways to determine the energy deposited in a material, *TID* and *Linear Energy Transfer* (LET). By definition, the change in kinetic energy per unit mass, dT/dm , is the TID, while the change in kinetic energy per unit path length, dT/dx , is the LET. Because the energy transfer per unit path length is dependent on the number of atoms encountered per unit

path length, both the TID and LET are seen to be dependent on target density. In addition to target density, the energy transfer is dependent on a parameter called the stopping cross section, which is defined by

$$\sigma_{stop} = \int \Delta T dA , \quad (5.5)$$

where ΔT is the kinetic energy lost by the particle moving through the area dA .

The cross sectional area of an object when viewed from a particular angle is the total area of the orthographic projection of the object from that angle. Therefore, in our specific case, the cross section concept is the total flux of particles that are incident to the spacecraft, seen from a determinate direction.

Thus, LET is seen to be given as

$$-\frac{dT}{dx} = n\sigma_{stop} . \quad (5.6)$$

LET is mainly a concern for SPEs and GCRs. The GCR flux defines the minimum background level seen. Any SPEs, no matter how large, increase the background level.

The selection of satellite's materials is determined by the LET values that it has to endure on orbit. That fact is due to each material having a different LET threshold and some materials showing more resistance than others. These LET values are in turn dependent on the environment. Therefore, depending on satellite's orbit parameters it has different expected thresholds.

One important issue is that semiconductors have trended toward smaller dimensions and smaller voltages. However, in space conditions, these semiconductors will become more susceptible to radiation damage. Therefore, it is assumed that new technologies are not prepared to work in outer space, given that biggest semiconductor with high voltages perform better.

5.2.3.1. *SEE Due To GCR*

The GCR flux is composed of 85% H, 14% He, and 1% heavier ions (heavier ions are those which its atomic number is above 26, after Fe the other atoms are considered heavier ions), see Fig. 5.5. The TD due to GCRs is quite low, and the main effect of GCRs is to induce single-event phenomena in electronics.

The Earth's magnetic field must be penetrated by cosmic rays in order for them to reach a spacecraft in Earth orbit. The number of magnetic field lines a cosmic ray must cross to reach a given point within the magnetosphere approximately determines the minimum energy it must possess. Nevertheless, regions in the outer magnetosphere and near the poles can be reached at much lower magnetic rigidities than are required to reach points near the Earth's equator, due to the conversion of magnetic field lines, see Fig. 5.6.

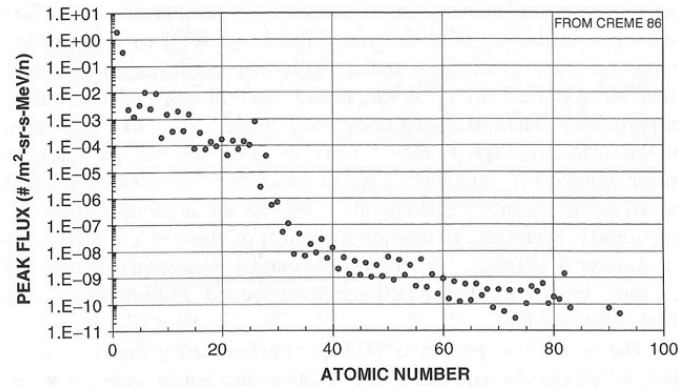


Fig 5.5 The relative abundances of all of the ions in cosmic rays. They are plotted in terms of the peak flux in their energy spectra.

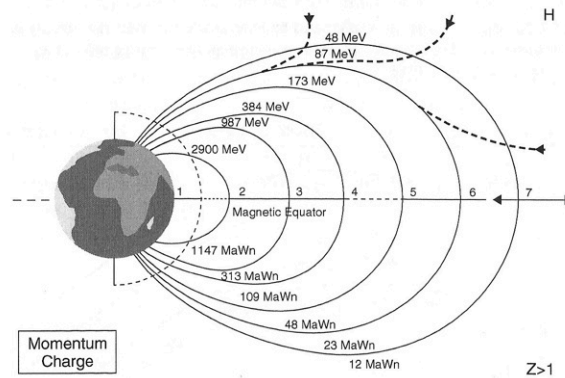


Fig. 5.6 Relationship between the dipole and cutoff rigidity to determine the particle energy required to penetrate the magnetosphere.

In order to determine the upset rates in space, we need to know how many ions deposit how much energy as they pass through the electronic chip. In order to do this we characterize the environment in terms of the number of ions as a function of their LET. We assume that all ions of a given LET will have the same effect.

Fig. 5.7 shows the total GCR LET spectrum. All of the ions heavier than hydrogen are included. However, the graph depicts that there exists a lower flux of the ions that have a bigger LET. Usually, those ions are the heavy ions. Moreover, we can see the difference between a solar maximum and a solar minimum and its effects on GCR collisions with spacecraft. The flux is much more important when the 11-year solar cycle goes through its minimum. An important point of this graph is that it takes into account a 100 mil of Al shielding.

It is important to cover satellites with shielding in order to stop some radiation damage. Nevertheless, an important shielding for radiation is Earth's magnetosphere. It can be stated that it is the most effective shielding for satellites, as it can be much more efficient than an aluminum covering.

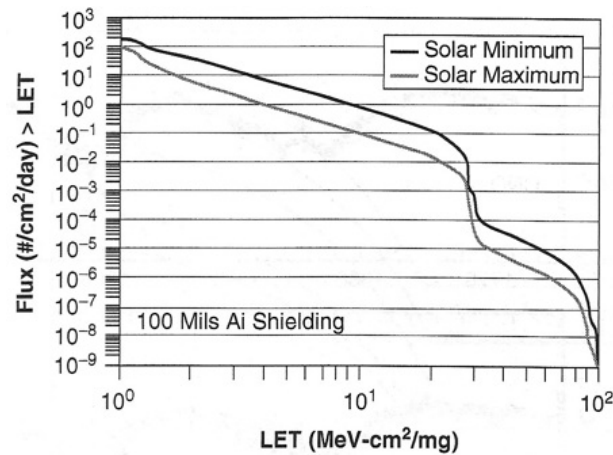


Fig. 5.7 Integral LET spectra for galactic cosmic rays during solar maximum and solar minimum.

Due to that fact, the ion's energy is lower as we move closer to the Earth. Moreover, depending on the inclination, the magnetosphere becomes stronger, being more effective in low inclination orbits. In Fig. 5.8 we can see that due to Earth's magnetic field, depending on the inclination, the flux of particles changes. The particle's flux is lower at orbits with zero inclination. Contrariwise, it becomes stronger as we increase the orbit inclination. Thus, polar orbits are subject to more intense fluxes. Apart from Earth's magnetosphere shielding, this study is also under 100 mils of aluminum shielding.

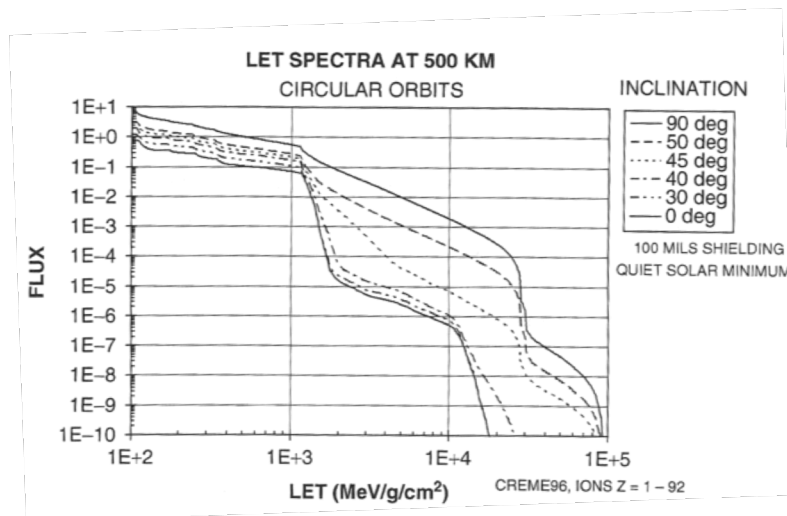


Fig. 5.8 Variation of LET spectra with inclination for LEO.

As it is stated before, Earth's magnetosphere is a natural shielding for satellites. Nevertheless it is also possible to build an artificial shielding, usually composed by Aluminum. This also helps to stop GCR to produce SEE in electronics. Figure 5.9 depicts how the flux decreases as the Al shielding increases.

As we can see it isn't as much effective as the Earth magnetic field, but it is able to reduce the flux of GCR. More or less, we can decrease an order of magnitude the flux with 5000 mils of Al shielding.

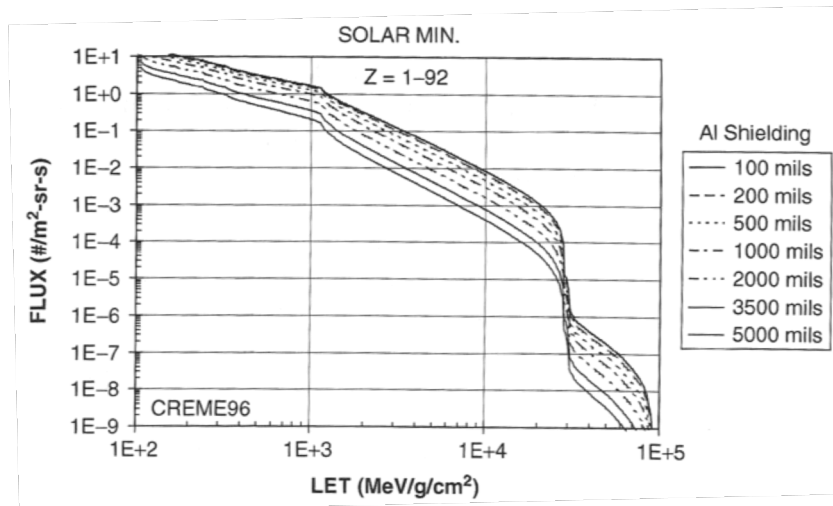


Fig. 5.9 Effect of shielding on cosmic ray LET spectra.

5.2.3.2. *SEE Due To Van Allen trapped particles*

At the previous paragraphs it is discussed the radiation effects due to heavy ions. However, for many low earth orbit heavy ions are a minor concern. Instead, the upsets due to particles in the Van Allen Belts, especially those in the SAA are of concern.

The trapped radiation belts are composed of energetic particles mostly electrons and protons, which are confined to gyrate around the Earth's magnetic field lines because the magnetic field constrains their motion. Van Allen belts are divided in two. The twin electron belts peaks are commonly referred to as the inner and outer belt, while the valley between them is called the slot region. The inner belt contains a fairly stable population of protons with energies exceeding 10 MeV. The outer belt contains mainly electrons with energies up to 10 MeV. Although the radiation belts are often thought of as being static, they exhibit temporal and spatial variation. Temporal variation arises because the radiation belts, which are controlled by the Earth's magnetic field, respond to geomagnetic storms and solar cycle. Spatial variations are due to the day/night asymmetry in the Earth's magnetic field at higher altitudes.

Depending on the orbit inclination and altitude the total exposure differs. Fig. 5.10 shows the proton fluency that exists for orbits in the radiation belt. At low altitudes the exposure occurs only in the SAA. Nevertheless, the proton's impacts increases when satellites go through the radiation belt until getting the peak-flux altitude. Moreover, proton's flux depends on the orbit inclination. Orbits contained in the equator plane encounter the biggest flux. However, the flux decreases in function of orbital inclination, being polar orbits the ones that experiment less impacts.

To mitigate the proton flux effects, satellites are covered by Aluminum shielding. As it is depicted in Fig. 5.11, the impacts are substantially reduced. With 500 mils of Aluminum shielding impacts are reduced one order of magnitude. However, if we

need to achieve a nearly perfect shielding, with 5000 mils of Aluminum the spacecraft reduces the proton's dose close to zero.

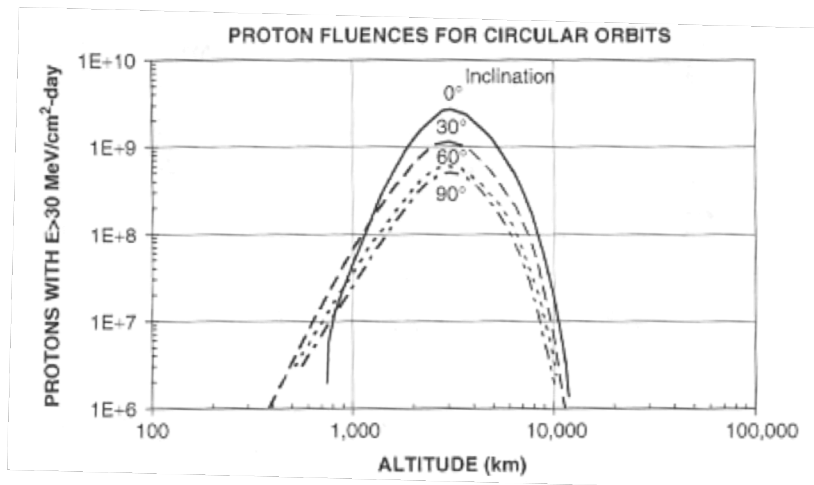


Fig. 5.10 Total exposure to trapped protons as a function of altitude and inclination for circular orbits.

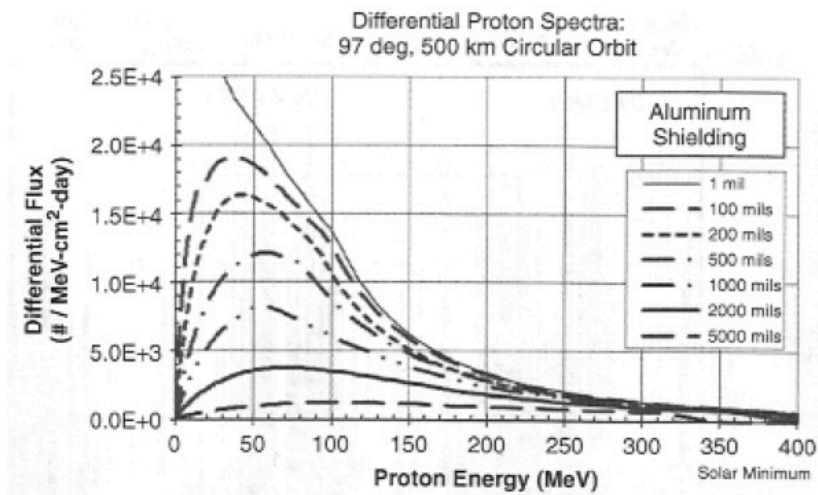


Fig. 5.11 Proton spectrum in low earth orbit showing the effect of aluminum shielding.

CHAPTER 6. SPACE TECHNOLOGY QUALIFICATION: EXPERIMENTAL TESTS

In this chapter we present the test and simulation results to space-qualify the microprocessor. In the previous chapter, we have shown all the theoretical aspects in order to better understand the results presented in this chapter. First, the results given by a test in a thermal vacuum chamber are presented. Then, the simulated results using two different software packages to predict the total dose experienced by the Arduino are analyzed.

6.1. Vacuum Test

The first test that the ATmega is submitted is to a vacuum test. This test consists on checking the Arduino performances under vacuum conditions, i.e., in a non-pressurized environment. To achieve this specific environment a thermal vacuum chamber is used. The vacuum chamber used for the experiments is depicted in Fig.6.1. This chamber belongs to the department of Signal Theory and Communications of the Universitat Politècnica de Catalunya. The Arduino is placed inside the vacuum chamber connected to a battery to get the necessary power to do the calculations.



Fig.6.1 Thermal Vacuum Chamber.

In order to check the Arduino performances, specific software is developed. This software basically performs mathematical computations and stores the results in an output file that is written on a SD card. For more information about the software see Appendix A. The results in the SD card reflect all the mathematical operations done by the microprocessor. Therefore, if any error exists in the processes, the output file will point them. This would translate into the fact that the Arduino does not stand this environment conditions.

During the experimental analysis in the laboratory, we frequently checked the vacuum chamber pressure. The LEDs mounted in the Arduino board showed whether it was working under normal conditions or not (see Appendix A). We check the LEDs in every sampling time, and they showed no problems during the whole test. Fig. 6.2 depicts the change in pressure in a logarithmic scale as a function of time. The slope change near 500 mbar is because the turbopump was turned on. Besides, we can see that the chamber is depressurized quickly until about 1,3 mbar. After that, the pressure decreases more slowly. In that moment, outgassing begins; the particles of gas accumulated in the Arduino become evaporated.

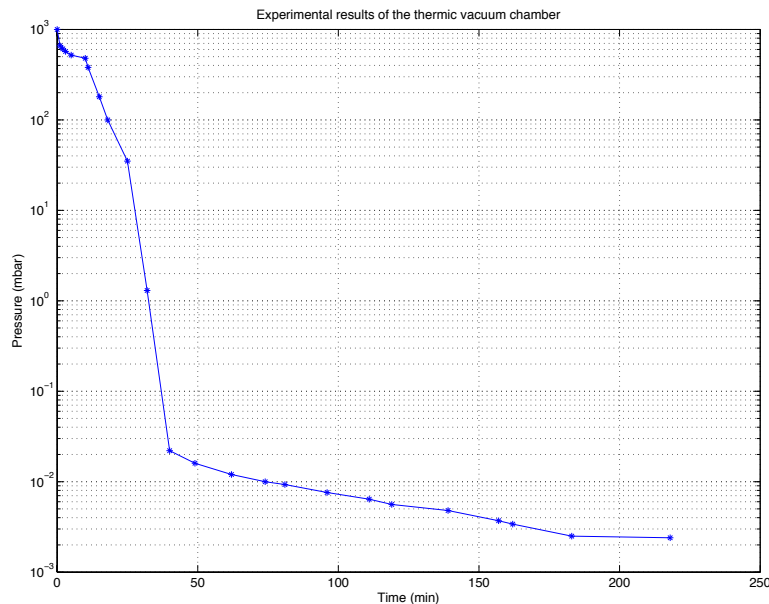


Fig. 6.2 Final test results.

Finally, after the test, we analyzed whether the Arduino had some problems on the calculations. We can see the exact results from the SD card in Appendix A. They confirm that the Arduino had overcome the vacuum test with no problems.

6.2. Temperature Test

In the temperature test we followed the same steps as in the vacuum test. We placed the Arduino inside the chamber, the LEDs were checked to assure the proper function of the board and the pressure was decreased. However, the thermal source was pointed towards the board after 180 minutes of test running. During 30 minutes the microprocessor was exposed to very low pressure and high temperature (with a 3 KW thermal source, depicted in Fig 6.3). We increased the temperature up to 50°C. The datasheet shows that the microprocessor should be able to work in good performance with temperatures up to 85°C. Nevertheless, this measure is provided in normal pressure conditions (sea level). Under this condition, convection phenomena help the microprocessor refrigerate itself. However, this phenomena are not present with the absent of pressure, and only radiation –and to a very limited extent conduction– are able to reduce the heat content of the Arduino. As a result, the maximum operating temperature in space would be lower than 85°C. As we can see from the output results the Arduino worked in perfect

performances during the whole period of time, and thus, it passed the test (see Appendix A).



Fig. 6.3 Thermal Source.

6.3. Radiation Test

Differing from the previous section, commercial software packages are used to evaluate the radiation that the board will experience. This is due to the high cost of the radiation experiment. Hence, the results shown in this section are simulated-based results instead of laboratory experimental ones. Hence, they can only offer an indication of the results that could be expected upon exposition to the space radiation environment; while this is obviously valuable information, it can only indicate in general terms whether the system could fail or not after a given time in low Earth orbit.

The effects of the Van Allen belts are simulated due to its high influence. Simulations will consider the use of different types of shielding in order to reduce the total dose on the microprocessor.

In order to simulate the interaction of the Van Allen belts, we use the AP-8 physical model for protons, and the AE-8 physical model for electrons. Some of their characteristics are shown in Table 6.1. In the simulations, the worst case of fluency is always used.

Table 6.1. Characteristics of the used physical models.

Parameters	AP-8 protons	AE-8 electrons
Maximum Energy	400 MeV	7 MeV
Minimum Energy	0,1 MeV	0,04 MeV
Maximum Flux on Orbit (LEO) at a height of	1900 km	1900 km

GCR differs strongly from the results obtained in simulations to the real measurements in outer space. As a consequence, GCR are not simulated in this thesis due to its low reliability results.

Nowadays there are different software packages that allow us to simulate space environments and its effects in electronics without the need to perform real experiments in laboratory or in outer space. Therefore, the cost is considerably reduced. However, it remains mandatory that simulation results should be contrasted with real data experiments.

In order to choose the proper software package, it is useful to analyze their performances and capabilities. The ones that best fit the requirements and needs of this project are the FLUKA and the SPENVIS.

6.3.1. FLUKA

FLUKA is a fully integrated particle physics MonteCarlo simulation package [14] [15]. It has many applications in high-energy experimental physics and engineering, shielding, detector and telescope design, cosmic ray studies, dosimetry, medical physics and radiobiology. FLUKA is a general purpose tool for calculations of particle transport and interactions with matter, covering an extended range of applications spanning from proton and electron accelerator shielding to target design, calorimetry, activation, dosimetry, detector design, Accelerator Driven Systems, cosmic rays, neutrino physics, radiotherapy etc. [16].

In this thesis we are going to use FLAIR [17]. FLAIR is an advanced user-friendly interface for FLUKA to facilitate the editing of FLUKA input files, execution of the code and visualization of the output files. A basic FLUKA tutorial is developed in Appendix B.

In order to simulate the radiation due to trapped belts with FLUKA, we check the interaction of an electron and a proton beam with a slab of silicon that represents the microprocessor. The shielding effects are also analyzed.

ELECTRON BEAM

First we are going to study the total equivalent dose on the Arduino without shielding. This simulation considers an electron beam. Besides, it considers that particles have the maximum possible energy in the Van Allen belts according to AE-8 physical model.

Fig.6.4 shows the amount of secondary radiation that is created after the interaction with silicon. This radiation is of big concern due to its high energy and low velocity. Because of that, it can produce important damage to electronics. This radiation is formed by principally muons and pions. As we can see from Fig. 6.4 (d), the radiation increases while passing through the silicon slab. However, we can see that it is less than 6 pSv for a 10.000 particles flux.

After that, the response of shielding in front of an electron beam is analyzed. Different materials for shielding with different thickness configurations are considered.

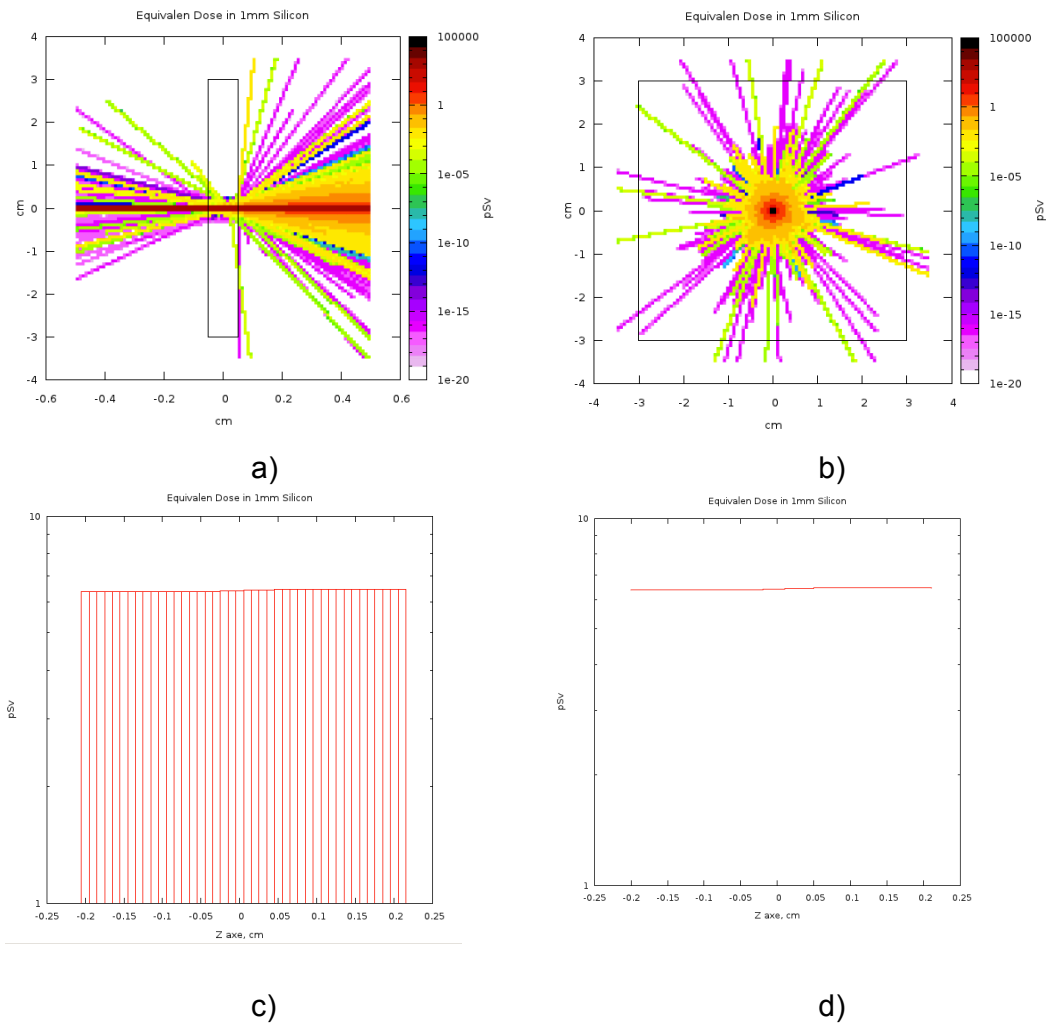
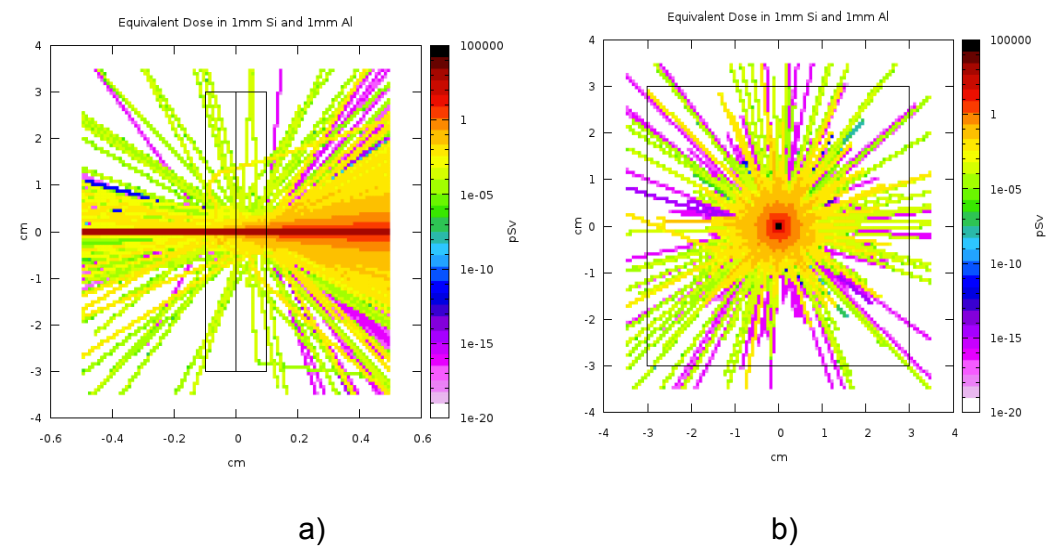


Fig.6.4 FLUKA Total Equivalent Dose in 1mm Si (from -0,05 cm to 0,05 cm), electron beam. a) 2D projection, seen from Z axe. b) 2D projection, seen from Y axe. c) 1D projection, boxes. d) 1D projection, steps.



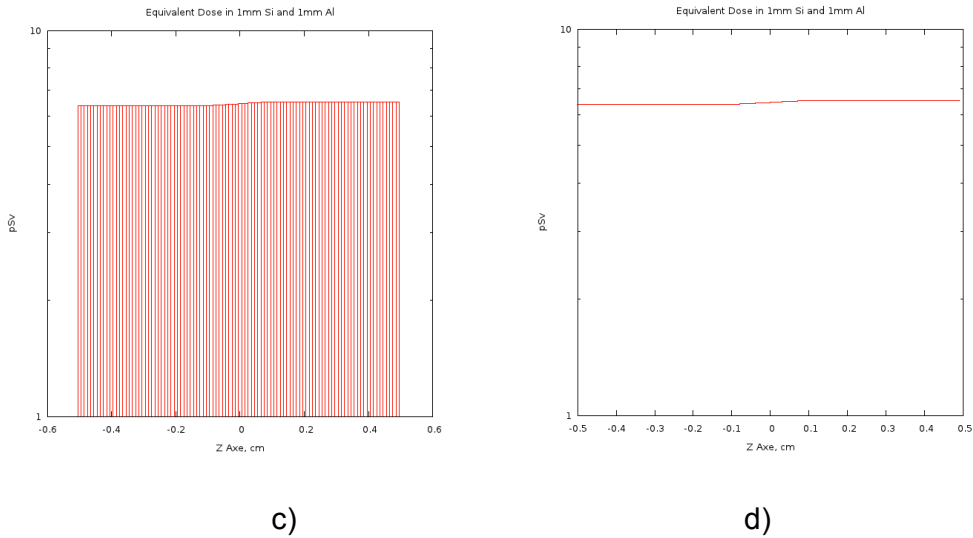
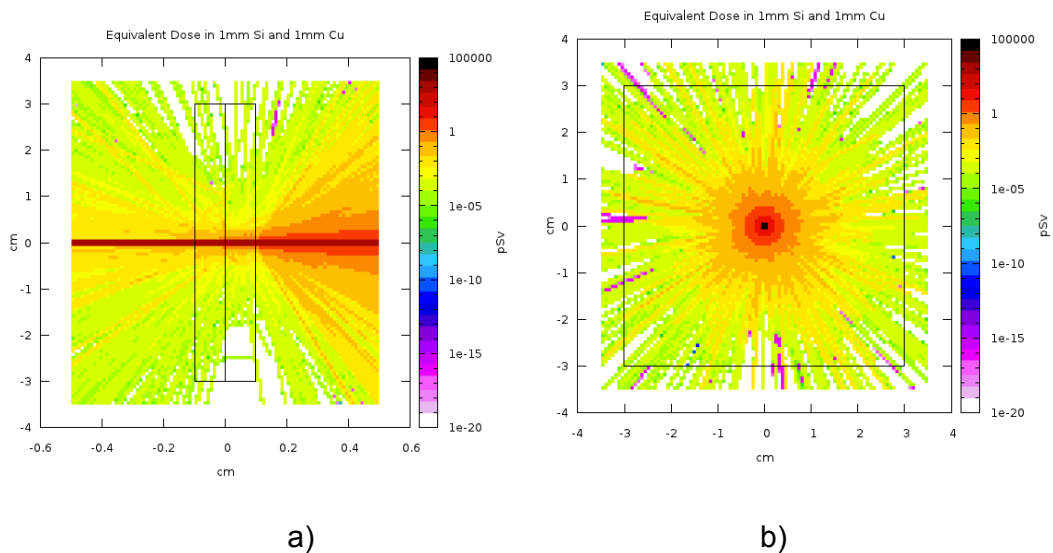


Fig.6.5 FLUKA Total Equivalent Dose in 1mm Si (from 0 to 0,1cm) and 1mm Al (from -0,1 to 0 cm), electron beam. a) 2D projection, seen from Z axe. b) 2D projection, seen from Y axe. c) 1D projection, boxes. d) 1D projection, steps.

Fig. 6.5 (a) and (b) show that the secondary radiation is increased as a consequence of using aluminum shielding. This secondary radiation produces an increase of total equivalent dose in the silicon.

For that reason, we study another shielding to compare which one would be better to protect the Arduino. Copper is the other shielding candidate.



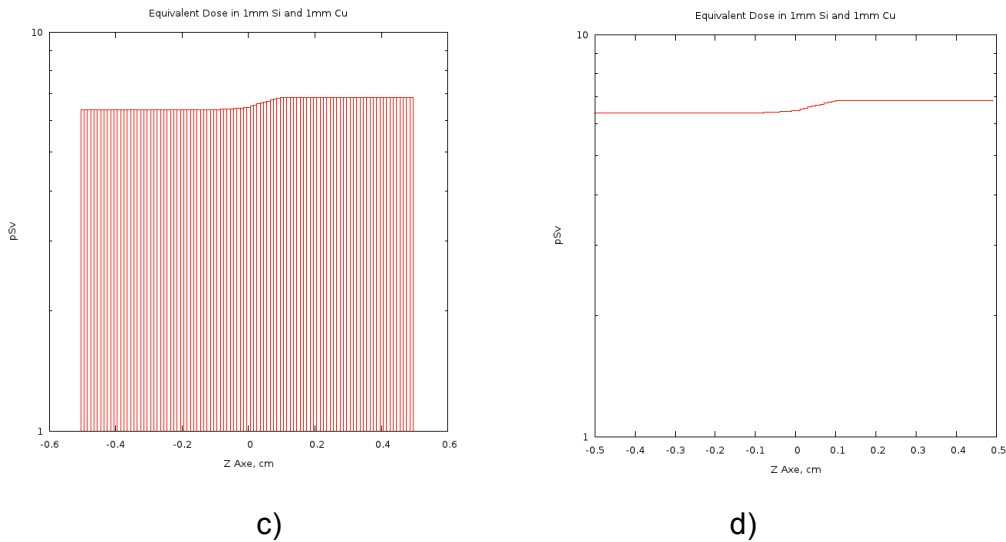
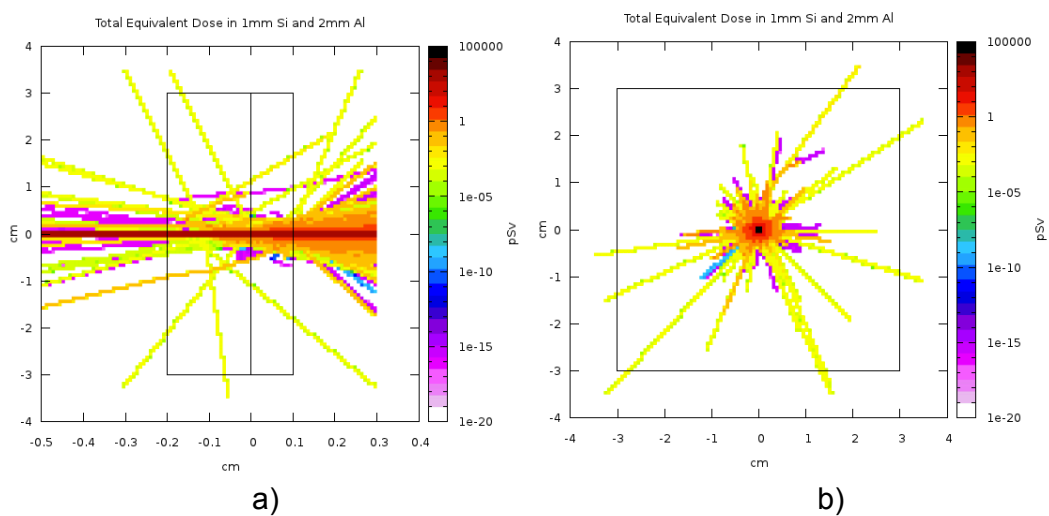


Fig.6.6 FLUKA Total Equivalent Dose in 1mm Si (from 0 to 0,1 cm) and 1mm Cu (from -0,1 to 0 cm), electron beam. a) 2D projection, seen from Z axe. b) 2D projection, seen from Y axe. c) 1D projection, boxes. d) 1D projection, steps.

If we compare the two different shieldings we conclude that the aluminum shielding is more effective than copper since aluminum keeps the secondary radiation lower than copper. Fig.6.6 shows that the total equivalent dose is increased up to approximately 7 pSv when using the copper shielding, and 6 pSv when aluminum is used (see Fig. 6.5). This is not a big difference but in a long period of time it could be crucial for the microprocessor.

As a result, we will use aluminum for the rest of the simulations. Fig. 6.7 and Fig. 6.8 present the differences between the thicknesses of shielding.



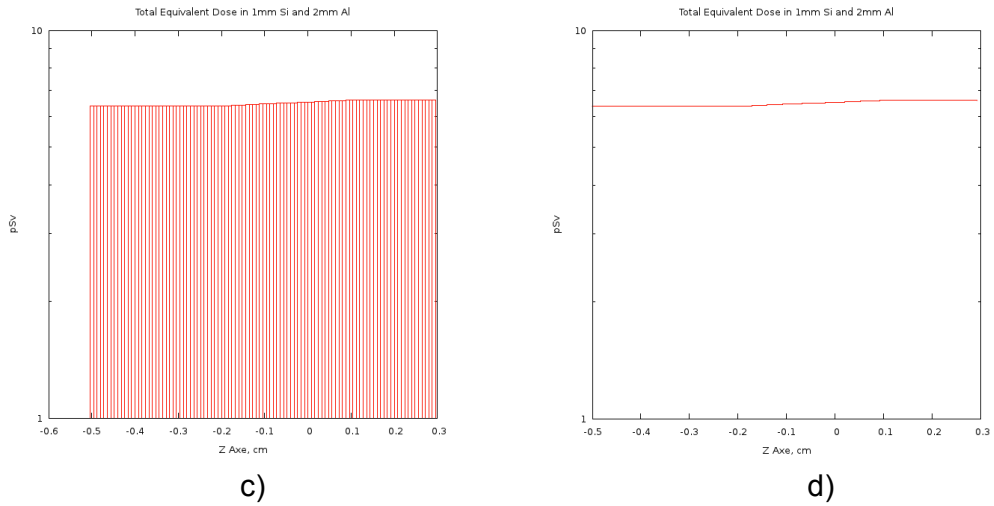
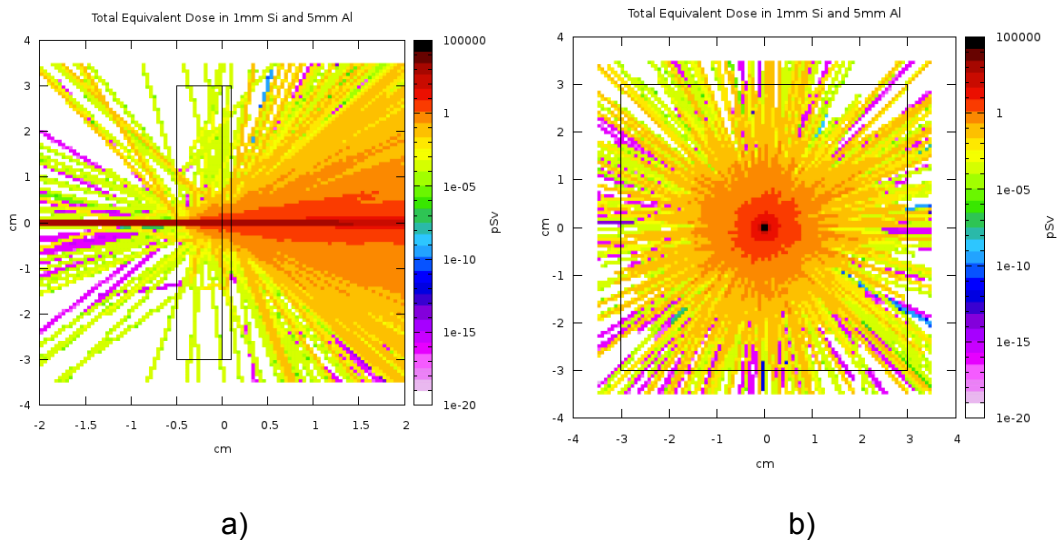


Fig.6.7 FLUKA Total Equivalent Dose in 1mm Si (from 0 to 0,1 cm) and 2mm Al (from -0,2 to 0 cm), electron beam. a) 2D projection, seen from Z axe. b) 2D projection, seen from Y axe. c) 1D projection, boxes. d) 1D projection, steps.

As it was commented before, Fig. 6.7 and Fig. 6.8 show that by increasing the thickness of the aluminum shielding, the secondary radiation gets higher and as a result the total dose increases.

We can conclude that aluminum does not provide good performances in front of electrons. It reduces primary radiation at the cost of producing secondary radiation. Both radiations can cause severe damages on the microprocessor if they achieve a dose high enough. Therefore, we must find a thickness that balances both radiations.



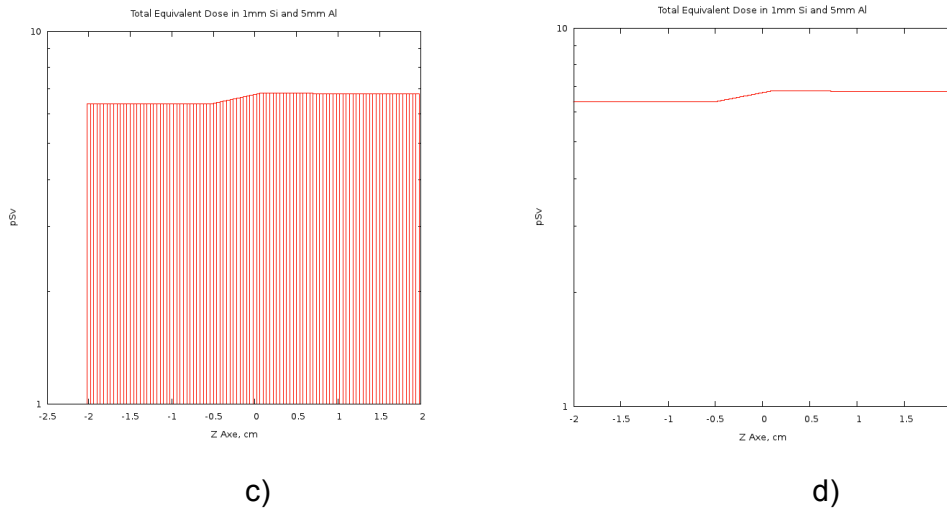


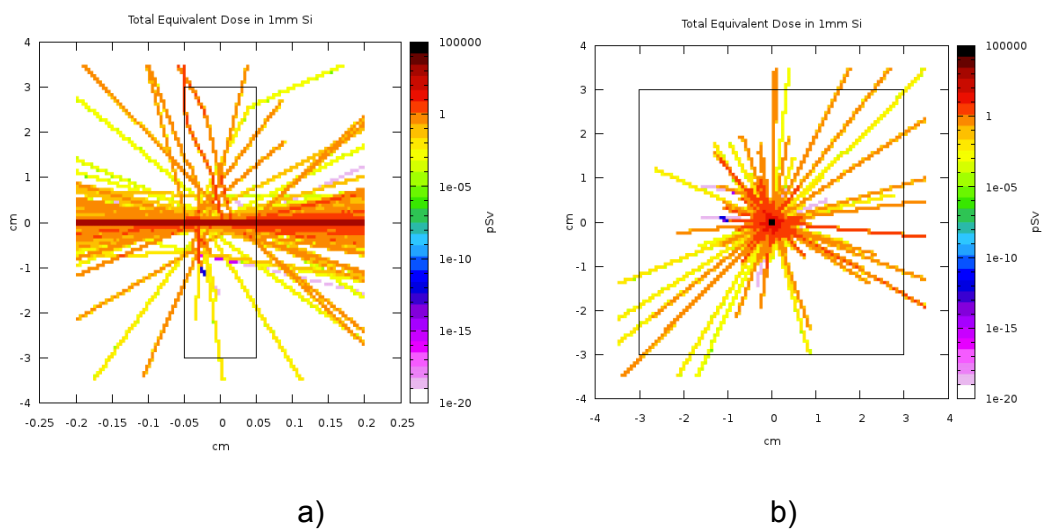
Fig.6.8 FLUKA Total Equivalent Dose in 1mm Si (from 0 to 0,1cm) and 5mm Al (from -0,5 to 0 cm), electron beam. a) 2D projection, seen from Z axe. b) 2D projection, seen from Y axe. c) 1D projection, boxes. d) 1D projection, steps.

PROTON BEAM

In this section, protons are studied in order to simulate the whole interaction in the Van Allen belts. Protons are more energetic particles than electrons and can cause more damage to the processor.

The analysis carried out in this section is similar to the one previously presented for the case of electrons.

First we will analyze the direct proton beam to silicon. Results are shown in Fig. 6.9.



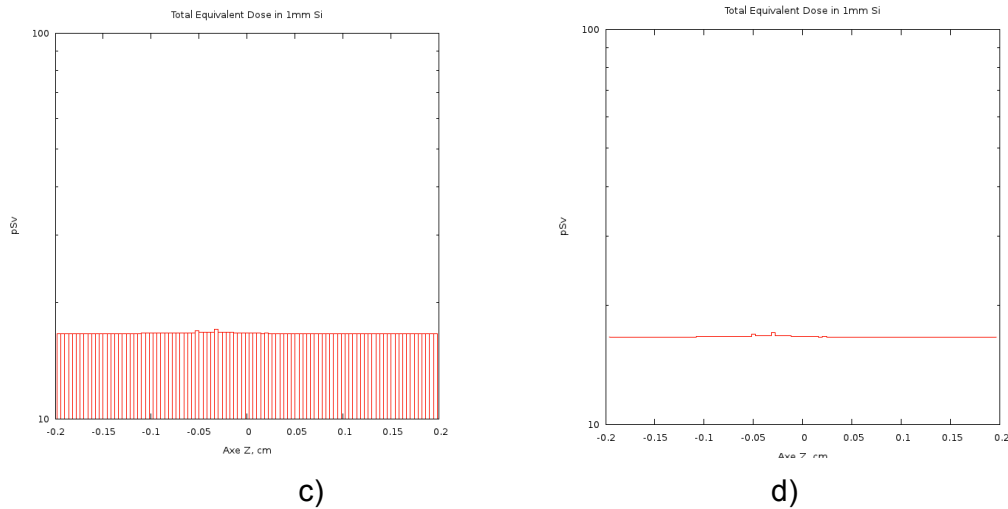
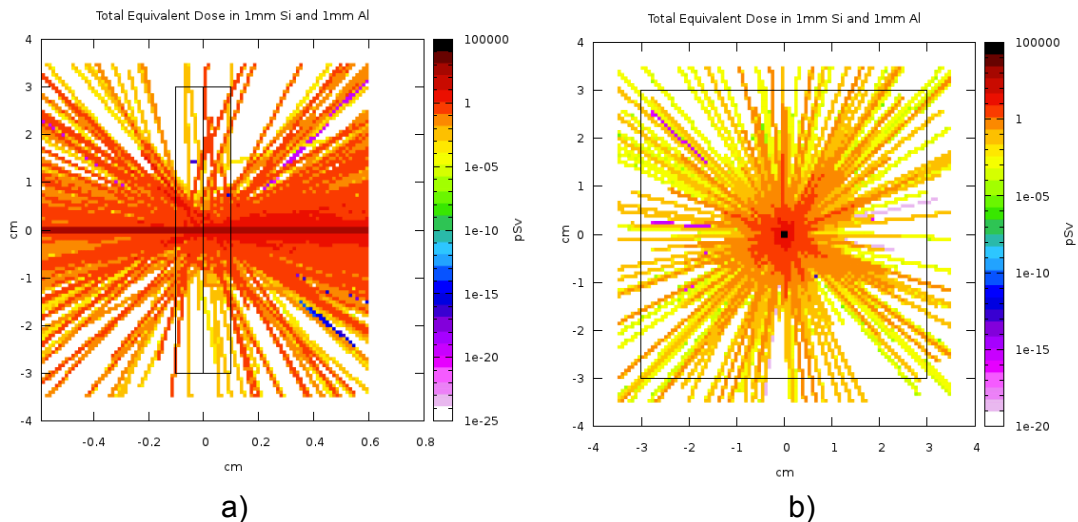


Fig.6.9 FLUKA Total Equivalent Dose in 1mm Si (from -0,05 to 0,05 cm), proton beam. a) 2D projection, seen from Z axe. b) 2D projection, seen from Y axe. c) 1D projection, boxes. d) 1D projection, steps.

As we can see the total equivalent dose due to protons in the trapped belts is higher than the total equivalent dose found in the previous section where electrons were considered.

Now, the response of the shielding in front of a proton beam is analyzed. Fig. 6.10 depicts the influence of a proton beam in the silicon. Since protons do not create as much as secondary radiation as electrons, the shielding shows an effective response because the total equivalent dose is reduced. As a conclusion, the microprocessor is more protected from radiation effects.



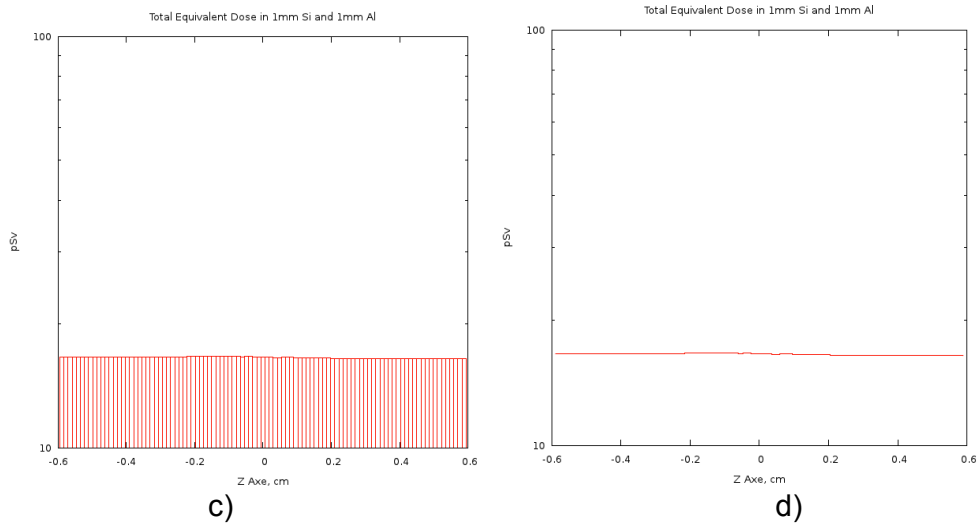
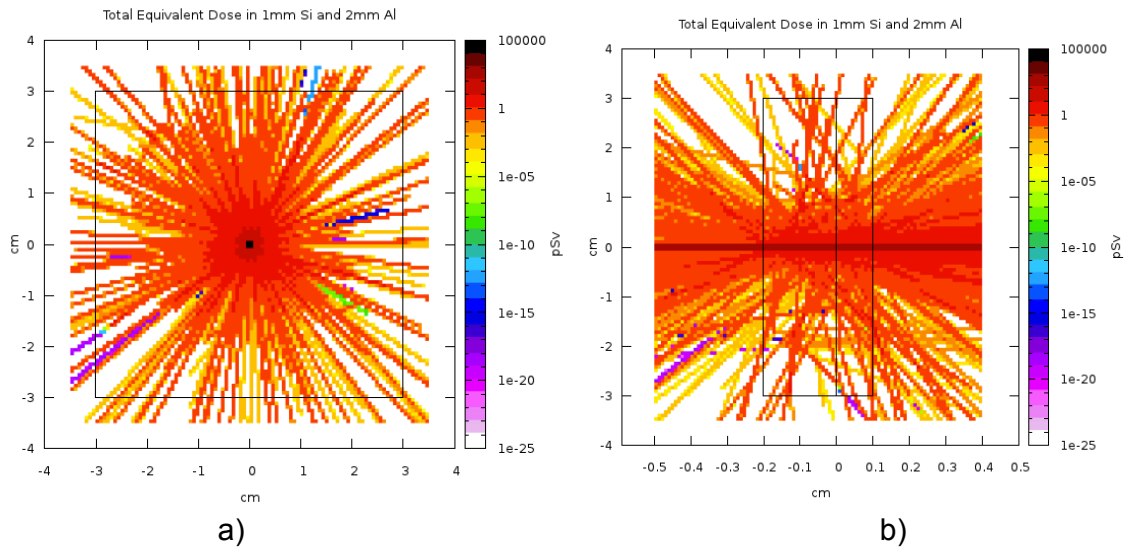


Fig.6.10 FLUKA Total Equivalent Dose in 1mm Si (from 0 to 0,1 cm) and 1mm Al (from -0,1 to 0 cm), proton beam. a) 2D projection, seen from Z axe. b) 2D projection, seen from Y axe. c) 1D projection, boxes. d) 1D projection, steps.

As it is depicted in Fig. 6.11, by means of increasing the thickness of the aluminum shielding, the total dose in the silicon slat is reduced.



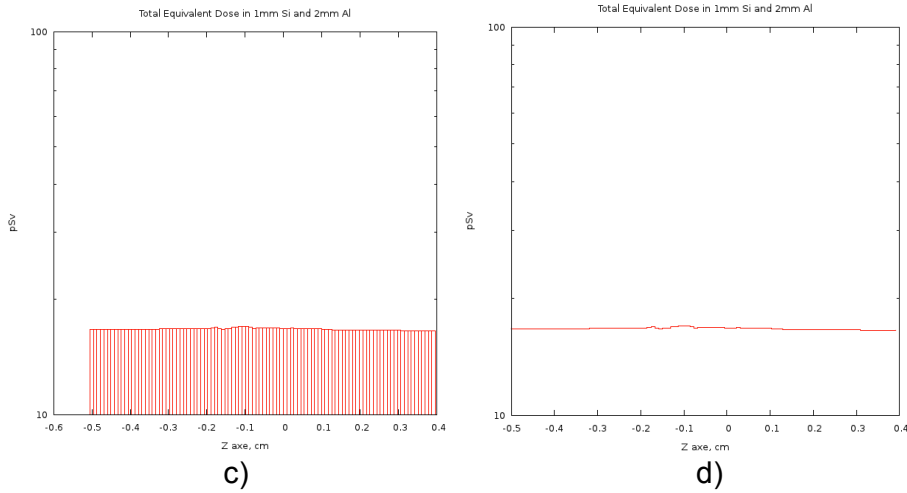
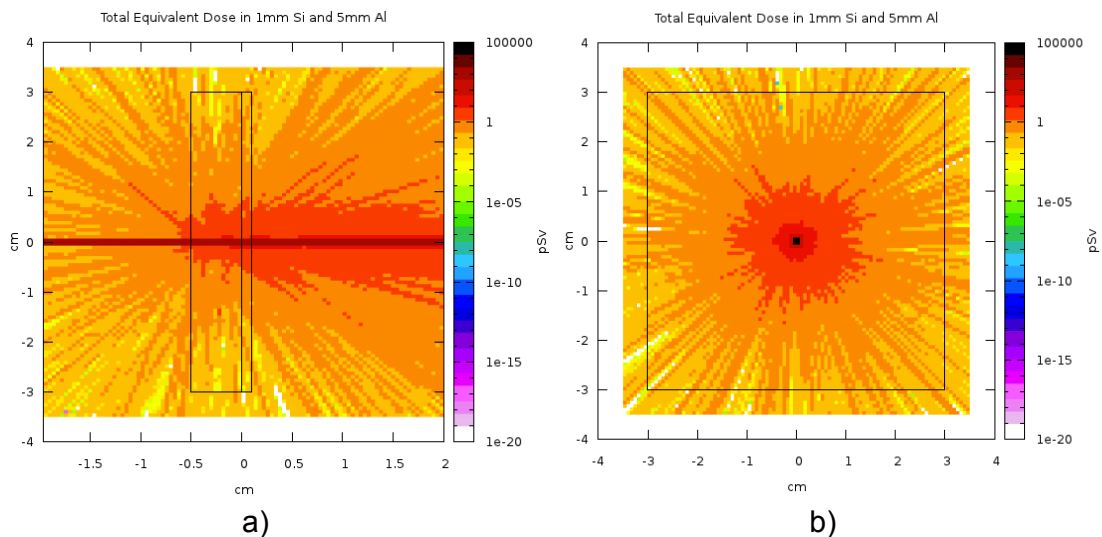


Fig. 6.11 FLUKA Total Equivalent Dose in 1mm Si (from 0 to 0,1 cm) and 2mm Al (from -0,2 to 0 cm), proton beam. a) 2D projection, seen from Z axe. b) 2D projection, seen from Y axe. c) 1D projection, boxes. d) 1D projection, steps.

Finally, Fig. 6.11 and 6.12 compare 2 mm and 5 mm of Aluminum shielding. We can see that the radiation is considerably reduced when using the 5 mm shielding, as it was expected. As a consequence, the microprocessor is much protected from radiation. However, by increasing the thickness of shielding, the total satellite weight is also increased. Launching a high-weight satellite requires a high-cost mission. As a result, there exists a trade-off between protection in front of radiation and total cost mission.



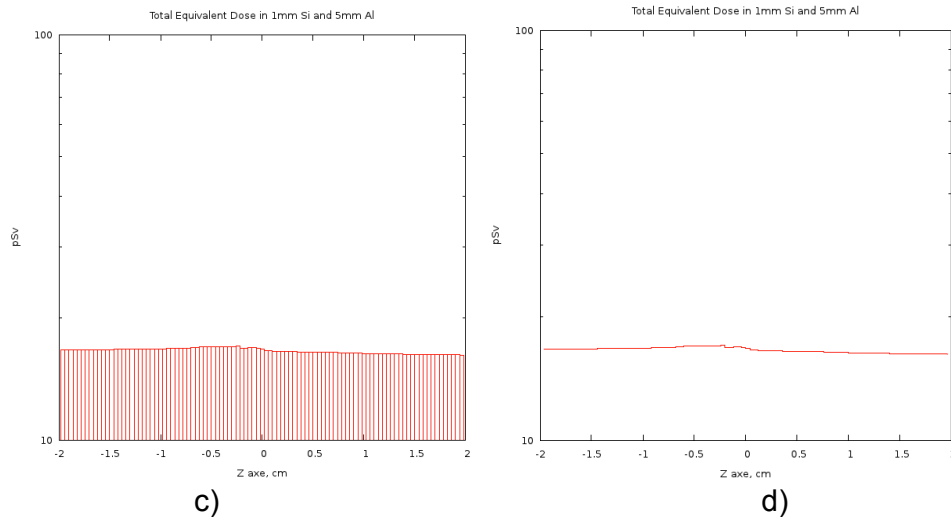


Fig. 6.12 FLUKA Total Equivalent Dose in 1mm Si (from 0 to 0,1 cm) and 5mm Al (from -0,5 to 0 cm), proton beam. a) 2D projection, seen from Z axis. b) 2D projection, seen from Y axis. c) 1D projection, boxes. d) 1D projection, steps.

After the analysis of shielding using FLUKA we can confirm that it is effective in front of protons because it reduces the total accumulated dose. Nevertheless, it is not too much crucial for electrons.

Total dose of protons must be added together with the total dose due to electrons to evaluate the total dose that the microprocessor may get due to Van Allen belts.

6.3.2. SPENVIS

In this section, we perform a similar radiation analysis with a different software. The Space Environment Information System (SPENVIS) is an ESA operational software developed and maintained at Belgian Institute for Space Aeronomy since 1996 [18]. It provides a web-based interface for assessing the space environment and its effects on spacecraft systems and crews. The system is used by an international scientific community for various purposes. For example, mission analysis and planning, educational support, and running models for scientific applications. SPENVIS also includes extensive background information on the space environment and the environment models.

ELECTON BEAM

As in the previous section, we start the total dose analysis with an electron beam and we change the type and thickness of shielding as well.

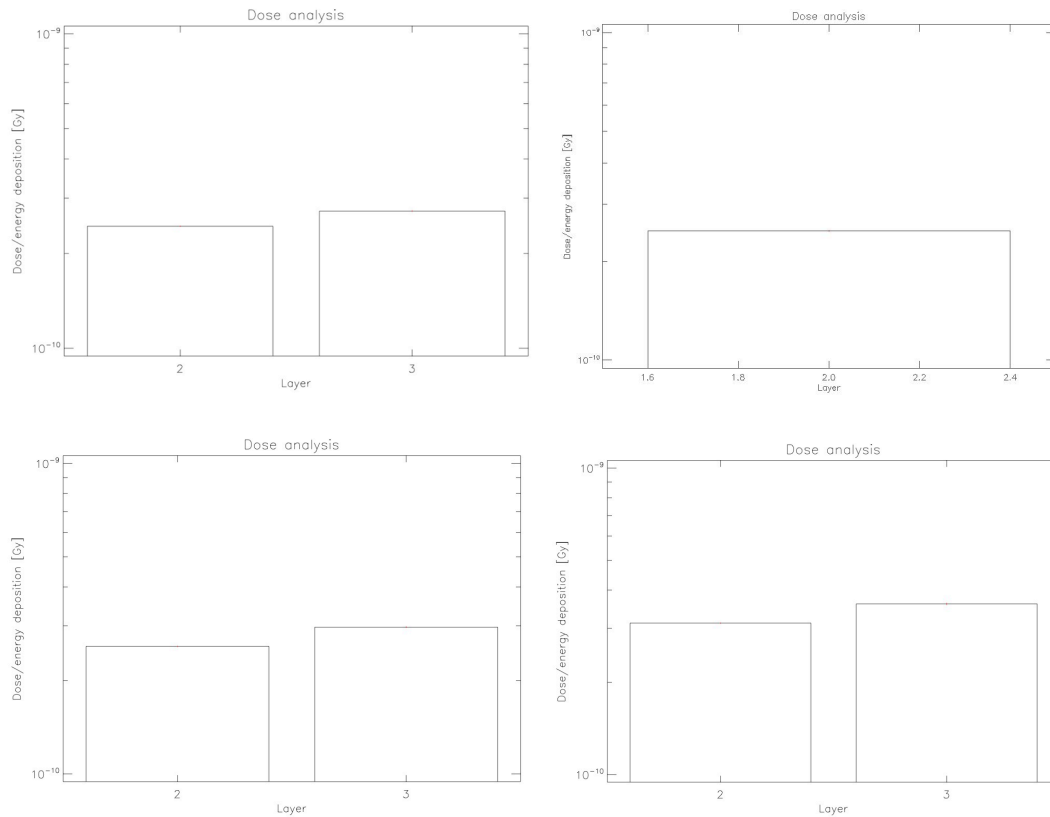


Fig. 6.13 SPENVIS, electron beam simulations. a) Total Ionizing Dose in 1mm Si, b) Total Ionizing Dose in 1mm Al (layer 2) and 1mm Si (layer 3), c) Total Ionizing Dose in 2 mm Al (layer 2) and 1mm Si (layer 3), d) Total Ionizing Dose in 5 mm Al (layer 2) and 1mm Si (layer 3).

As we saw previously with FLUKA, the simulation showed that the Total Dose due to electrons in Silicon increased with shielding. This was due to the creation of secondary radiation produced by the shielding itself.

If we analyze Fig. 6.13, we can see that the units used in both software programs differ. In FLUKA simulations, the results were presented with Sv, which is a SI unit. However, in SPENVIS does not show the option to show results with this unit. Therefore, Gy are used. This unit differs from the former one depending on the radiation source and the target material. Nevertheless, since a proton and an electron beam are considered, we can assume that Gy and Sv provide the same results.

Moreover, another difference is that in SPENVIS we concentrate the whole particles beam in a 1 cm^2 . Nevertheless, FLUKA perform the simulations considering the whole geometry. Therefore, taking into account that FLUKA geometry is 36 cm^2 , the results concentrate the beam in this 36 cm^2 . Hence, there exists a considerable difference between them.

However, by means of adding a normalization factor in FLUKA, we are able to compare both results and then analyze the total dose. For example if the electron beam is analyzed in a slat of 1mm Si using FLUKA, we get $6,5 \cdot 10^{-12} \text{ Sv}$ approximately. The result obtained using SPENVIS is $2,5 \cdot 10^{-10} \text{ Gy}$. By dividing the

results found with SPENVIS, $2,5 \cdot 10^{-10}$ Gy, with the geometry difference between the two targets (of both softwares), i.e., $25 \cdot 10^{-9}$ Gy/ 36 cm^2 , the result is $6,9 \cdot 10^{-12}$ Gy. As it was mentioned before, since two units (Gy and Sv) are totally equivalent for this case, we can conclude that both software suites give us a close result.

If we take a look at the other graphs and results the difference between them is the same. We need to normalize the FLUKA results by the size of the used geometry, i.e., 36 cm^2 .

PROTON BEAM

Proton fluency was previously analyzed with FLUKA. Now, we are going to perform the same simulations with SPENVIS in order to compare the results.

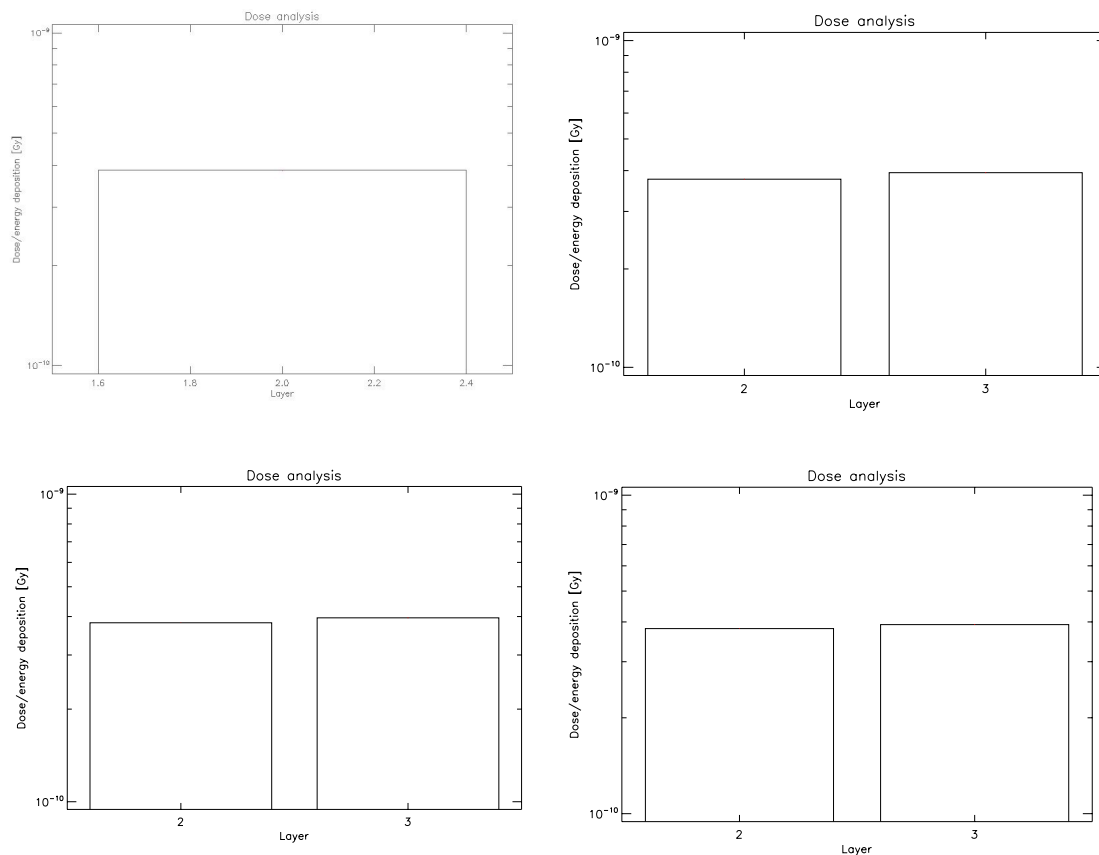


Fig. 6.14 SPENVIS, proton beam simulations. a) Total Ionizing Dose in 1mm Si, b) Total Ionizing Dose in 1mm Al (layer 2) and 1mm Si (layer 3), c) Total Ionizing Dose in 2 mm Al (layer 2) and 1mm Si (layer 3), d) Total Ionizing Dose in 5 mm Al (layer 2) and 1mm Si (layer 3).

Fig. 6.14 depicts the interaction of protons in silicon with different types of shielding. As we saw in the previous section with FLUKA, the shielding was more effective with protons than with electrons. Nevertheless, in SPENVIS simulations, the radiation in silicon (with shielding) does not decrease as happen in Fig 6.10 and Fig 6.11. Now, the silicon reaches the same level of dose as aluminum, without being decreased.

6.3.3. Conclusions

Finally, we only need to conclude what the total dose that the Arduino would experiment is. As we mentioned before total dose coming from electrons and protons must be added to get the real total dose. The results are shown in Table 6.2.

Table 6.2. Original results.

		FLUKA (TD in Si) Sv	SPENVIS (TD in Si) Gy
ELECTRON	1mm Si	$6,5 \cdot 10^{-12}$	$2,5 \cdot 10^{-10}$
	1mm Al + 1mm Si	$6,6 \cdot 10^{-12}$	$2,7 \cdot 10^{-10}$
	2mm Al + 1mm Si	$6,7 \cdot 10^{-12}$	$3 \cdot 10^{-10}$
	5mm Al + 1mm Si	$6,9 \cdot 10^{-12}$	$3,5 \cdot 10^{-10}$
PROTON	1mm Si	$16 \cdot 10^{-12}$	$3,8 \cdot 10^{-10}$
	1mm Al + 1mm Si	$15,7 \cdot 10^{-12}$	$4 \cdot 10^{-10}$
	2mm Al + 1mm Si	$15,5 \cdot 10^{-12}$	$4 \cdot 10^{-10}$
	5mm Al + 1mm Si	$15,1 \cdot 10^{-12}$	$4 \cdot 10^{-10}$

Table 6.3 shows the result after making the normalization in FLUKA in order to know the particles per 1 cm^2 without the interaction of the geometry.

Table 6.3. Normalized results.

		FLUKA (TD in Si) Sv	SPENVIS (TD in Si) Gy
ELECTRON	1mm Si	$2,3 \cdot 10^{-10}$	$2,5 \cdot 10^{-10}$
	1mm Al + 1mm Si	$2,37 \cdot 10^{-10}$	$2,7 \cdot 10^{-10}$
	2mm Al + 1mm Si	$2,4 \cdot 10^{-10}$	$2,9 \cdot 10^{-10}$
	5mm Al + 1mm Si	$2,5 \cdot 10^{-10}$	$3,5 \cdot 10^{-10}$
PROTON	1mm Si	$5,6 \cdot 10^{-10}$	$3,8 \cdot 10^{-10}$
	1mm Al + 1mm Si	$5,7 \cdot 10^{-10}$	$3,9 \cdot 10^{-10}$
	2mm Al + 1mm Si	$5,5 \cdot 10^{-10}$	$3,9 \cdot 10^{-10}$
	5mm Al + 1mm Si	$5,4 \cdot 10^{-10}$	$3,9 \cdot 10^{-10}$

Table 6.4 presents the total dose that the microprocessor intercepts.

Table 6.4. Final TD results.

		FLUKA (TD in Si) Sv	SPENVIS (TD in Si) Gy
PROTON + ELECTRON	1mm Si	$7,9 \cdot 10^{-10}$	$6,3 \cdot 10^{-10}$
	1mm Al + 1mm Si	$8,0 \cdot 10^{-10}$	$6,6 \cdot 10^{-10}$
	2mm Al + 1mm Si	$7,9 \cdot 10^{-10}$	$6,8 \cdot 10^{-10}$
	5mm Al + 1mm Si	$7,9 \cdot 10^{-10}$	$7,4 \cdot 10^{-10}$

By looking at the previous tables, it is concluded that FUKA does not vary the total dose as a function of shielding. After considering some possibilities of this phenomenon, we concluded that, the secondary radiation created by electrons was so intense that shielding was not efficient, that is, by increasing the shielding, the primary radiation decreases but the secondary radiation increases. At the end, the accumulated total dose is conserved and no gain due to shielding is experienced.

On the other hand, the simulation results found with SPENVIS says that the accumulated total dose increases when the thickness of the shielding also increases. This may be due to the importance of the secondary radiation.

Now, we need to study whether the Arduino would survive those radiation levels. We know that, generally, COTS technology is able to resist about 50-100 Sv of radiation. Therefore, given the results of total dose provided in the previous tables, we can confirm that the microprocessor could work in a similar environment during a rather long period of time.

CHAPTER 7. CONCLUSIONS AND FUTURE WORK

In this chapter we present the final conclusions after all the theoretical studies and the experimental results. We also present some future works that can extend the work carried out in this thesis.

7.1. Conclusions

This thesis has considered the advance in TRL of a commercial microprocessor, the Atmega 168. This processor is included in the femtosatellite being developed at EETAC.

A motivation and introduction of the thesis was presented in Chapter 1, jointly with an outline of the work.

Chapter 2 presented the main features of the processor and its main potential mission applications. This description was needed to achieve TRL levels 1 and 2.

In order to achieve TRL level 3, some laboratory experiments and computer simulations were carried out. The microprocessor was exposed to high temperatures and low-pressure environments to qualify it in extreme conditions found in outer space. The experiment was conducted in a thermal vacuum chamber. The microprocessor showed good performances with 50°C of temperature and pressures close to zero (at these pressures there is an absent of convection mechanisms that would help the processor to get colder).

Then, radiation analysis was studied by means of commercial software FLUKA and SPENVIS. The interaction of the particles deposited at the Van Allen belts were addressed and total dose effects results were extracted. We contrasted the results of both packages. FLUKA showed that by using shielding, the accumulated radiation levels are not reduced. The primary radiation is indeed decreased, but at a cost of increasing the secondary radiation. At the end, the accumulated total dose is conserved and no gain due to shielding is experienced. On the other hand, SPENVIS results showed that the total dose radiation increases even when shielding is present. This may be due to the importance of the secondary radiation.

However, generally, COTS technology is able to resist about 50-100 Sv of radiation. Therefore, given the results of total dose provided in Chapter 6, we can confirm that the microprocessor could work in a similar environment during a certain period of time.

Given all that, we can conclude that the microprocessor has achieved TRL level 3. It passed all the tests and simulations conducted in this thesis.

TRL 4 is not achievable because the integration of the rest of the satellite components was not considered in this work.

7.2. Future Work

There are some extensions that can be carried out this work. We suggest the following points:

- To conduct radiation experiments with electron/proton beams to contrast the results obtained in the simulations.
- More realistic and complete experiments may be considered, with longer durations of expositions.
- Testing components under critical/risky situations.
- The integration with other satellite components, and the testing of the proper work of the integration needs to be done to achieve TRL level 4.

BIBLIOGRAPHY

- [1] https://telecom.esa.int/telecom/media/document/TRL_Handbook.pdf
- [2] <http://www.atmel.com/Images/doc2545.pdf>
- [3] <http://arduino.cc/it/Main/ArduinoBoardProMini>
- [4] Joshua Tristancho, *Implementation of a femtosatellite and a mini-launcher*, Universitat Politècnica de Catalunya, Barcelona, 2010.
- [6] Allan C. Tribble, *The Space Environment*, Princeton University Press, 1995.
- [7] P. Fortescue, J. Stark, G. Swinerd, *Space System Engineering*, Willey, 2003.
- [8] <http://www.haystack.mit.edu/atm/science/thermo/index.html>
- [9] E. Petersen, *Single Event Effects in Aerospace*, Willey, 2011.
- [10] James C. Pickel, "Single Event Effects Rate Prediction", *IEEE*, Vol.43, No. 2, p.483-495, 1996.
- [11] Craig I. Underwood, "The Single Event behaviour of Commercial-Off-The-Shelf memory devices-a decade in Low-Earth Orbit", *IEEE*, Vol.45, No.3, p.1450-1457, 1998.
- [12] Roben A. Reed et al, "Single. Event Effects ground testig and on.orbit rate precton methods: the past, present, and future", *IEE*, Vol.50, No. 3, p. 622-634, 2003.
- [13] Stefano Bertazzoni et al, " TID and SEE characterization and damaging analysis of 256 Mbit COTS SDRAM for IEEM application", *RADECS*, p.11-1 – 11-4, 2005.
- [14] G. Battistoni, S. Muraro, P.R. Sala, F. Cerutti, A. Ferrari, S. Roesler, A. Fassò, J. Ranft, "The FLUKA code: Description and benchmarking" *Proceedings of the Hadronic Shower Simulation Workshop 2006*, Fermilab 6-8 September 2006, M. Albrow, R. Raja eds., AIP Conference Proceeding 896, 31-49, (2007).
- [15] A. Ferrari, P.R. Sala, A. Fassò, and J. Ranft "FLUKA: a multi-particle transport code" , *CERN-2005-10 (2005)*, INFN/TC_05/11, SLAC-R-773.
- [16] <http://www.fluka.org>

[17] <http://www.fluka.org/flair/index.html>

[18] <http://www.spenvis.oma.be/>

APPENDIX A.

The software used in the experiments calculates the prime numbers and then checks the results obtained comparing them with a database. After that, it saves all the results in an SD memory card.

Code:

http://dl.dropbox.com/u/4774705/programa_V2_SD_final3.pde

Moreover, you can obtain the P_e , the number of total trials, failures and successes.

Before all the experimental results, we tested the Arduino in the laboratory environment, with ambient pressure and temperature. As we can see in the following video links the Arduino software works properly. In this videos it is explained how to upload the software to the Arduino, board, how to connect it to the battery and how to get the final results form its SD card.

Video 1:

<http://dl.dropbox.com/u/4774705/MOV00149.AVI>

Video 2:

<http://dl.dropbox.com/u/4774705/MOV00151.AVI>

Output file validation:

<http://dl.dropbox.com/u/4774705/OUTPUT.DataValidation.pdf>

In order to test the software, we changed the prime numbers database to check if Arduino would find a failure. The results are in the Output file failure validation. As we can see, it finds the error.

Output file failure validation:

<http://dl.dropbox.com/u/4774705/OUTPUTDataValidationFailure.pdf>

Finally, the final results of the vacuum and temperature tests are found in:

<http://dl.dropbox.com/u/4774705/OUTPUT.DataValidation.pdf>

Moreover, output file validation, output file failure validation and final output are found at the end of the thesis.

APPENDIX B.

FLAIR is an advanced user-friendly interface for FLUKA to facilitate the editing of FLUKA input files, execution of the code and visualization of the output files. Coming up, a beginner's FLUKA tutorial is developed.

When initializing FLAIR the main window and the output window will appear:



Fig. B.1. FLAIR output window.

The output window presented in Fig. B.1 displays all information that is printed on the standard output and standard error unit. Flair is always writing the commands that are executed. If some problem occurs output window shows more information.

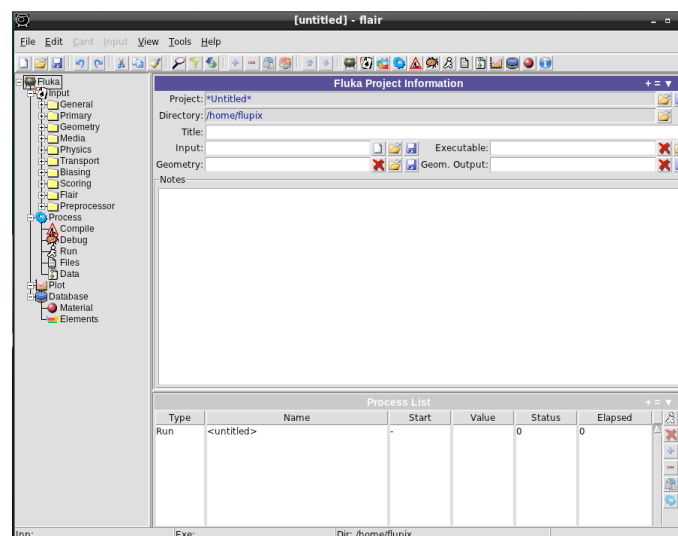


Fig. B.2 FLAIR main window.

FLAIR main window, depicted in Fig. B.2, shows the menu on top, a tool-bar with icons for fast access and status bar at the bottom to display some useful information for the current frame. Also there are two frames, left frame is a tree browser for the various sections of the project. The right frame encapsulates the entire project frames used for editing the information stored in the project file.

Main window has some different options. In this window, you choose the project name, directory and title. Moreover, you can choose a specific template for the project. Nevertheless, it is also possible to create a new project without any kind of template. An important issue is that FLUKA lets you use an external geometry file.

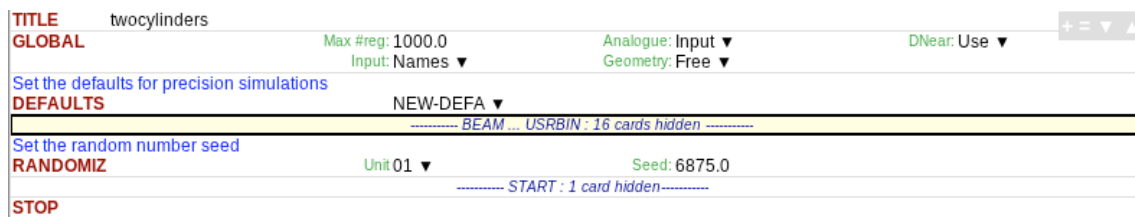


Fig. B.3 FLAIR general window.

The next step is following with general window (Fig. B.3) where the general program characteristics are chosen. The basic ones are TITLE, GLOBAL (this function makes a global declaration about the present run, setting important parameters that must be defined before array memory allocation). Also you choose the type of format in the geometry input bodies and regions. Another important function is START. It defines the termination condition, gets a primary from a beam or from a source and starts the transport.



Fig. B.4 FLAIR primary window.

After that, primary window is shown Fig. B.5. In this window all the beam performances are defined. All "events" or "histories" are initiated by primary particles. The card BEAM defines all the characteristics of the particles energy (or momentum), shape, distribution, etc. while the card BEAMPOS controls their starting position and direction.



Fig. B.6 FLAIR geometry window.

In the window shown in Fig. B.6, the geometry of our project can be created in case we do not pick up an external geometry file. The input for the Combinatorial Geometry (bodies, regions and optional region volumes) must be immediately preceded by a GEOBEGIN card and immediately followed by a GEOEND card. The whole geometry must be surrounded by a region of "blackhole" limited by a closed body (generally an RPP parallelepiped). It is also useful to surround the actual geometry by a region of ideal vacuum, and to have the blackhole region surrounding the vacuum. This can be useful, for instance, in order to start the trajectory of the primary particles outside the physical geometry (a particle may not be started on a boundary).



Fig. B.7 FLAIR media window

In the window shown in Fig. B.7 the media is chosen, that means, the different materials of the experiment are uploaded to the geometry. FLAIR has a large variety of different materials. Finally, in the Scoring window Fig. B.8 users set the simulation that they need. Some options are USRTRACK, which defines a detector for a track-length fluency estimator. On the other hand, URSCOLL defines a detector for a collision fluency estimator. URSYIELD defines a detector to score a double-differential particle yield around an extended or a point target. And USRBIN scores distribution of one of several quantities in a regular spatial structure, binning detector, independent from the geometry.

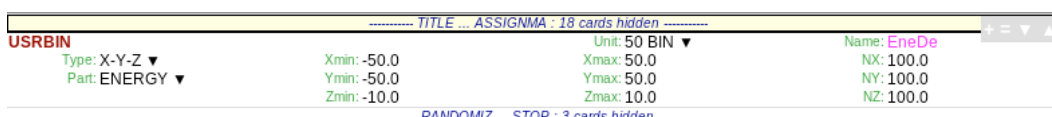


Fig. B.8 FLAIR scoring window.